MODIFICATION OF PALLADIUM SURFACES BY ELECTROCHEMICAL ATOMIC LAYER DEPOSITION (E-ALD) AND ATOMIC LAYER ELECTROLESS DEPOSITION (ALED) FOR ENHANCED HYDROGEN TRANSPORT KINETICS

by

DAVID MICHAEL BENSON, JR.

(Under the Direction of John Stickney)

ABSTRACT

Applications that rely on hydrogen storage and exchange, such as sensors, catalysis, and energy storage, can be improved by increasing the rate at which hydrogen can be both stored and accessed. Pd is a well-known candidate for hydrogen storage and exchange purposes. In this lab, surface modification of Pd films by Rh deposition using electrochemical atomic layer deposition (E-ALD), a condensed-phase equivalent of atomic layer deposition (ALD), has been shown to enhance the rates of hydrogen sorption and desorption into and out of the Pd film. Using a new columnar flow cell design, this deposition technique has been applied to Pd powder. Modified powders were studied using cyclic voltammetry, scanning transmission electron microscopy with energy dispersive X-ray spectroscopy (STEM-EDS), and X-ray photoelectron spectroscopy (XPS). An analogous electroless deposition technique, atomic layer electroless deposition (ALED), uses hydrogen rather than a metal as the sacrificial element and has also been adapted to the flow cell system. Deposits of Pd and Rh on a Pd substrate were created. Films grown in the flow cell by E-ALD and ALED were compared by cyclic

voltammetry and by voltammetric stepping. Another electroless deposition technique, electroless atomic layer deposition (EL-ALD) is presented. EL-ALD uses redox couples in solution to poise the potential at a desired voltage to promote underpotential deposition (UPD) of a metal which then acts as a sacrificial layer to deposit another desired metal. Results and future directions are presented.

INDEX WORDS: E-ALD, SLRR, UPD, ALED, CV, Pd, Rh, Pt, electrochemistry, thin film, flow cell, electrochemical atomic layer deposition, underpotential deposition, atomic layer, electroless, hydrogen absorption, adsorption

MODIFICATION OF PALLADIUM SURFACES BY ELECTROCHEMICAL ATOMIC LAYER DEPOSITION (E-ALD) AND ATOMIC LAYER ELECTROLESS DEPOSITION (ALED) FOR ENHANCED HYDROGEN TRANSPORT KINETICS

by

DAVID MICHAEL BENSON, JR.

BS, Saint Vincent College, 2010

A Dissertation Submitted to the Graduate Facility of The University of Georgia in Partial Fulfillment of the Requirements for the Degree

DOCTOR OF PHILOSOPHY

ATHENS GA
2015

© 2015

David Michael Benson, Jr.

All Rights Reserved

MODIFICATION OF PALLADIUM SURFACES BY ELECTROCHEMICAL ATOMIC LAYER DEPOSITION (E-ALD) AND ATOMIC LAYER ELECTROLESS DEPOSITION (ALED) FOR ENHANCED HYDROGEN TRANSPORT KINETICS

by

DAVID MICHAEL BENSON, JR.

Major Professor: John L Stickney

Committee: I. Jon Amster

Tina Salguero

Electronic Version Approved

Suzanne Barbour
Dean of the Graduate School
The University of Georgia
December 2015

DEDICATION

To my family.

Mom, Dad, Kelly, Kathryn, and Rachelle, without your encouragement, love, and support, this would have never been possible.

ACKNOWLEDGEMENTS

I would like to acknowledge John Stickney for opening his group to me. His guidance will remain with me always. I cannot overstate how grateful I am, not only for the opportunity he gave me, but also for all of the wisdom he shared so freely. I would also like to thank the current and prior members of the Stickney group. They have been a continuous source of support and friendship. Finally, I also owe my gratitude to Jeff Urbauer, without whom I would not have made it this far.

TABLE OF CONTENTS

Page

ACKNOWLEDGEMENTS……………………………………………………………….v

CHAPTER

1. INTRODUCTION AND LITERATURE REVIEW……………………………...1
2. ENHANCED KINETICS OF ELECTROCHEMICAL HYDROGEN UPTAKE AND RELEASE ON PALLADIUM POWDERS MODIFIED BY ELECTROCHEMICAL ATOMIC LAYER DEPOSITION………………….....13
3. ATOMIC-LAYER ELECTROLESS DEPOSITION IN A FLOW CELL………53
4. HYDROGEN SORPTION KINETICS OF PALLADIUM NANOFILMS MODIFIED WITH RHODIUM DEPOSITED BY ELECTROCHEMICAL ATOMIC LAYER DEPOSITION (E-ALD) AND ATOMIC LAYER ELECTROLESS DEPOSITION (ALED)…………..…....….…….……….….…73
5. ELECTROLESS ATOMIC LAYER DEPOSITION……………………….......89
6. CONCLUSION AND OUTLOOK………………………………………….106

CHAPTER 1

INTRODUCTION AND LITERATURE REVIEW

Palladium is well known for its ability to reversibly and selectively store and discharge a large relative volume of hydrogen in ambient conditions.[1] Pd has been applied for use in hydrogen storage,[2] hydrogen sensing,[3,4] and fuel cell catalysis.[5,6] Research of each of these applications has shown that formation of surface layers of other metals can enhance chemical or electronic properties.[7-9]

Thin films are desirable both for different properties they often exhibit compared to those of bulk materials, and for the reduced cost from using less material. As such, the growth of thin films is an attractive target in industry and academia. Several methods exist for creating thin films with controlled thickness, including successive ionic layer deposition and reaction (SILAR),[10] chemical vapor deposition (CVD), physical vapor deposition (PVD), and electrodeposition, and atomic layer deposition (ALD).[11] Ideally, the resulting deposit would have a surface coverage of one monolayer (ML), defined as one adsorbate atom per substrate atom.

ALD is popular for its atomic level control over deposit thickness and its broad applicability in depositing a variety of metals on numerous substrates.[12] ALD uses gas-phase surface limited reactions which terminate once the substrate is fully covered, ensuring deposits no more than one atom in thickness. The conditions for using ALD are somewhat prohibitive, however, as ALD operates under vacuum at relatively high temperatures, usually greater than 100 ºC.[13] A condensed phase analog of ALD called

electrochemical atomic layer deposition (E-ALD) has been developed which operates under ambient temperature and pressure.[14]

E-ALD works based on the use of underpotential deposition (UPD),[15-17] an electrochemical form of surface limited reaction.[18-20] UPD occurs as a result of the favorable free energy of formation of a compound or alloy, where one element deposits on another at a potential prior to ("under", typically more positive for cations) the potential required to deposit upon itself. The UPD metal is then exchanged at open circuit for ions of a more noble metal in solution by a process called surface limited redox replacement (SLRR).[21-25] The deposition is performed as a series of steps such as solution flow, exchange, and blank rinse, to form a cycle. The cycle is repeated a desired number of times as part of a sequence to create deposits of desired thickness. E-ALD has been used to create numerous deposits, including compound semiconductors[20,26,27] and metal films.[24,28,29]

SLRR was used in this group to grow thin films of Pd and study the hydrogen sorption and desorption properties.[30] The kinetics of surface limited hydride adsorption onto, and bulk hydride absorption into the Pd are important in catalysis, hydrogen storage, and hydrogen sensing. Following studies suggesting that other metal surface layers on Pd modify the surface hydride properties compared to bare Pd and might enhance the kinetics of hydrogen absorption and desorption,[9,31,32] recent work developed a SLRR cycle for Pd surface modification with submonolayer amounts of Rh.[33] Results from that study showed that Rh-modification of the Pd thin films caused enhanced kinetics for both hydrogen absorption and desorption, evidenced by cyclic voltammetry

(CV). This presented an opportunity for further study of the kinetics with varied amounts of Rh, and to study other metals deposited on Pd for comparison.

While E-ALD allows for the deposition of a variety of metals, as an electrochemical technique it will always require electrical connection to the substrate in order to control the potential, and will require increased current proportional to surface area in order to create deposits. Electroless deposition, however, does not require external contact to a device to control the potential.[34] Therefore, an electroless method would be desirable for situations where metals are supported on non-conducting materials, and where surface area is high, such as for large quantities of powder. For this reason, a technique called atomic layer electroless deposition (ALED) has been introduced.[35]

ALED works similarly to E-ALD in that it results in controlled submonolayer growth of a metal as a result of exchange for a sacrificial element. In ALED, however, the sacrificial element is hydrogen. The use of a nonmetal sacrificial element was first reported by Nutariya, et al. using H_{UPD}.[36] Another method for electroless deposition of surface limited amounts of metal called electroless surface limited redox replacement (E-SLRR) was developed by Ambrozik, et al.[37,38] In E-SLRR, a UPD layer of sacrificial metal is deposited before exchanging with the metal ions of interest. ALED uses advantageous features from each of these methods: a nonmetal sacrificial element, and a fully electroless deposition process. Another issue to address with standard plating solutions for industrial electroless deposition is that they often contain a complex mixture of chemicals including complexing agents, reducing agents, stabilizers, and inhibitors.[39] It would be beneficial to make the electroless deposition solutions more environmentally

friendly and less expensive.[40] ALED meets these criteria as the solutions used contain only H_2SO_4 with hydrogen, and the metal ion to be deposited.

One more type of electroless deposition called electroless atomic layer deposition (EL-ALD) is introduced. EL-ALD uses easily reversible redox couples dissolved in solution to maintain a poised potential to form a UPD layer of a sacrificial metal to then exchange at open circuit for the desired more noble metal. Using these controlled growth reactions, EL-ALD offers another electroless method to control deposit thickness at the atomic layer level.

This dissertation describes aqueous solution based atomic layer deposition techniques, E-ALD, ALED, and EL-ALD, for Pd, Rh, and Pt growth in an automated electrochemical flow cell system (Electrochemical ALD, L.C.) on powdered Pd and planar Pd substrates. The flow cell system consisted of a variable speed pump, solenoid selection valve, solution reservoirs, potentiostat, and a three electrode flow cell (Figure 1.1). Sequencer 4.0 (Electrochemical ALD, L.C.) control software was used to control the flow cell system both manually and through programmed deposition cycles. The typical flow cell for planar films, used for the majority of the experiments, is described in Chapter 3. Chapter 2 used a new flow cell designed to contain powders.

Chapter 2 of this dissertation features the adaptation of E-ALD to a Pd powder substrate, building off of previous work where Rh deposition was used to enhance the kinetics of H sorption and desorption from Pd films.[33] A new flow cell design was implemented in order to allow the use of a powder, as was a method for immobilizing mg-scale quantities of powder for use in the traditional flow cell. Rh was deposited on the Pd powder by 1, 3, and 6 cycles of E-ALD. The resulting deposits were analyzed

using cyclic voltammetry (CV), X-ray photoelectron spectroscopy (XPS), scanning transmission electron microscopy with energy dispersive X-ray spectroscopy (STEM-EDS). Pt was also deposited and studied by XPS and STEM-EDS. Kinetics of hydrogen transport were shown to be enhanced by the presence of Rh on the powder surface for mg-scale quantities of powder. The Rh and Pt deposits were uniform over the surface of the powder particles regardless of surface morphology. The films grew thicker with increasing numbers of deposition cycles.

Chapter 3 of this dissertation demonstrates the adaptation of a recent technique, atomic layer electroless deposition (ALED), to the flow cell system.[35] A method for forming surface hydride using dissolved H_2 in solution was optimized to create a deposition cycle that could be repeated to form a sequence. Samples of Pd on Pd and of Rh on Pd created by ALED were analyzed by cyclic voltammetry and by linear sweep voltammetry to examine the kinetic characteristics and quantitative characteristics of the films. CV results are consistent with layer-by-layer deposition. Linear sweep voltammetry quantified the amount of deposition generated per growth cycle. ALED was determined to deposit Pd at a lower rate compared to E-ALD. The ALED technique was proved possible, however, in a flow cell, leaving room for future comparison to modified films generated by E-ALD.

Chapter 4 compares Rh-modified Pd films generated in the flow cell system using atomic layer electroless deposition (ALED) and electrochemical atomic layer deposition (E-ALD). Voltammetric stepping is used to examine the rate of hydrogen desorption from saturated films generated by both methods. Decay curve fitting from the voltammetric profiles showed that the hydrogen desorption process occurred was best fit

to a biexponential decay. The decay profile indicates that the process involves rapidly desorbing hydrogen initially, and quickly transitioning to a slower rate. This can likely be explained by hydrogen from the bulk structure of the Pd leaving rapidly, while the more stable surface hydride leaves more slowly. Surface modification with Rh increased the rate at which the hydrogen was desorbed across the Pd both by ALED and E-ALD, though more cycles of ALED were required to obtain the same rates as E-ALD, in agreement with the conclusion from Chapter 3 that ALED deposits less metal per cycle than E-ALD.

Finally, Chapter 5 of this dissertation exhibits preliminary studies of another deposition technique, electroless atomic layer deposition (EL-ALD). Redox couples in solution are explored as a method of setting a controlled potential for electroless UPD formation. Growth of Pt on Pd is demonstrated using a poised potential in blank solution before going to open circuit and exchanging the blank for a Pt ion solution. Electrolessly deposited UPD Cu is shown to be attained using a ferrocyanide/ferricyanide solution. Cyclic voltammetry of both the Pt grown on Pd from poised-potential blank and Pd exchanged for the electroless UPD Cu is shown.

References

(1) Dullaghan, C. A., Abys, J.A.: Electrodeposition of palladium and palladium alloys. In *Modern Electroplating*; C.A. Paunovic, J. A. A., Ed.; John Wiley, Inc.: New York, 2000; pp 483-554.

(2) Niessen, R. A. H.; Vermeulen, P.; Notten, P. H. L. The electrochemistry of Pd-coated MgySc(1-y) thin film electrodes: A thermodynamic and kinetic study. *Electrochimica Acta* **2006**, *51*, 2427-2436.

(3) Noh, J.-S.; Lee, J. M.; Lee, W. Low-Dimensional Palladium Nanostructures for Fast and Reliable Hydrogen Gas Detection. *Sensors* **2011**, *11*, 825-851.

(4) Yoon, J.-H.; Kim, B.-J.; Kim, J.-S. Design and fabrication of micro hydrogen gas sensors using palladium thin film. *Materials Chemistry and Physics* **2012**, *133*, 987-991.

(5) Kang, S.; Heo, P.; Lee, Y. H.; Ha, J.; Chang, I.; Cha, S.-W. Low intermediate temperature ceramic fuel cell with Y-doped BaZrO3 electrolyte and thin film Pd anode on porous substrate. *Electrochemistry Communications* **2011**, *13*, 374-377.

(6) Lai, B.-K.; Kerman, K.; Ramanathan, S. Methane-fueled thin film micro-solid oxide fuel cells with nanoporous palladium anodes. *Journal of Power Sources* **2011**, *196*, 6299-6304.

(7) Bartlett, P. N.; Marwan, J. The effect of surface species on the rate of H sorption into nanostructured Pd. *Physical Chemistry Chemical Physics* **2004**, *6*, 2895-2898.

(8) Chen, X.; Burda, C. The Electronic Origin of the Visible-Light Absorption Properties of C-, N- and S-Doped TiO2 Nanomaterials. *Journal of the American Chemical Society* **2008**, *130*, 5018-5019.

(9) Greeley, J.; Mavrikakis, M. Surface and Subsurface Hydrogen: Adsorption Properties on Transition Metals and Near-Surface Alloys. *The Journal of Physical Chemistry B* **2005**, *109*, 3460-3471.

(10) Pathan, H. M.; Lokhande, C. D. Deposition of metal chalcogenide thin films by successive ionic layer adsorption and reaction (SILAR) method. *Bulletin of Materials Science* **2004**, *27*, 85-111.

(11) Barlow, F., Elshabini-Riad, Aicha, Brown, R.: Film Deposition Techniques and Processes. In *Thin Film Technology Handbook*; McGraw-Hill: New York, 1997.

(12) Johnson, R. W.; Hultqvist, A.; Bent, S. F. A brief review of atomic layer deposition: from fundamentals to applications. *Materials Today* **2014**, *17*, 236-246.

(13) George, S. M. Atomic Layer Deposition: An Overview. *Chemical Reviews* **2009**, *110*, 111-131.

(14) Stickney, J. L. Electrochemical atomic layer epitaxy (EC-ALE): Nanoscale control in the electrodeposition of compound semiconductors. *Advances in Electrochemical Science and Engineering* **2002**, *7*, 1-106.

(15) Adzic, R. R.: Electrocatalytic Properties of the Surfaces Modified by Foreign Metal Adatoms. Wiley-Interscience: New York, 1984.

(16) Kolb, D. M.: Advances in Electrochemistry and Electrochemical Engineering. John Wiley: New York, 1978.

(17) Magnussen, O. M. Ordered Anion Adlayers on Metal Electrode Surfaces. *Chemical Reviews* **2002**, *102*, 679-726.

(18) Gregory, B. W.; Norton, M. L.; Stickney, J. L. Thin-layer electrochemical studies of the underpotential deposition of cadmium and tellurium on polycrystalline Au, Pt and Cu electrodes. *Journal of Electroanalytical Chemistry* **1990**, *293*, 85-101.

(19) Gregory, B. W.; Stickney, J. L. Electrochemical atomic layer epitaxy (ECALE). *Journal of Electroanalytical Chemistry* **1991**, *300*, 543-561.

(20) Gregory, B. W.; Suggs, D. W.; Stickney, J. L. Conditions for the Deposition of CdTe by Electrochemical Atomic Layer Epitaxy. *Journal of The Electrochemical Society* **1991**, *138*, 1279-1284.

(21) Herrero, E.; Buller, L. J.; Abruña, H. D. Underpotential Deposition at Single Crystal Surfaces of Au, Pt, Ag and Other Materials. *Chemical Reviews* **2001**, *101*, 1897-1930.

(22) Brankovic, S. R.; Wang, J. X.; Adžić, R. R. Metal monolayer deposition by replacement of metal adlayers on electrode surfaces. *Surface Science* **2001**, *474*, L173-L179.

(23) Mrozek, M. F.; Xie, Y.; Weaver, M. J. Surface-enhanced Raman scattering on uniform platinum-group overlayers: preparation by redox replacement of underpotential-deposited metals on gold. *Analytical chemistry* **2001**, *73*, 5953-5960.

(24) Kim, Y.-G.; Kim, J. Y.; Vairavapandian, D.; Stickney, J. L. Platinum Nanofilm Formation by EC-ALE via Redox Replacement of UPD Copper: Studies Using in-Situ Scanning Tunneling Microscopy. *The Journal of Physical Chemistry B* **2006**, *110*, 17998-18006.

(25) Vasilic, R.; Dimitrov, N. Epitaxial Growth by Monolayer-Restricted Galvanic Displacement. *Electrochemical and Solid-State Letters* **2005**, *8*, C173-C176.

(26) Banga, D. O.; Vaidyanathan, R.; Xuehai, L.; Stickney, J. L.; Cox, S.; Happeck, U. Formation of PbTe nanofilms by electrochemical atomic layer deposition (ALD). *Electrochimica Acta* **2008**, *53*, 6988-6994.

(27) Wade, T. L.; Ward, L. C.; Maddox, C. B.; Happek, U.; Stickney, J. L. Electrodeposition of InAs. *Electrochemical and Solid-State Letters* **1999**, *2*, 616-618.

(28) Sheridan, L. B.; Czerwiniski, J.; Jayaraju, N.; Gebregziabiher, D. K.; Stickney, J. L.; Robinson, D. B.; Soriaga, M. P. Electrochemical atomic layer deposition (E-ALD) of palladium nanofilms by surface limited redox replacement (SLRR), with EDTA complexation. *Electrocatalysis* **2012**, *3*, 96-107.

(29) Sheridan, L. B.; Gebregziabiher, D. K.; Stickney, J. L.; Robinson, D. B. Formation of Palladium Nanofilms Using Electrochemical Atomic Layer Deposition (E-ALD) with Chloride Complexation. *Langmuir* **2013**, *29*, 1592-1600.

(30) Sheridan, L. B.; Kim, Y.-G.; Perdue, B. R.; Jagannathan, K.; Stickney, J. L.; Robinson, D. B. Hydrogen adsorption, absorption, and desorption at palladium nanofilms formed on Au (111) by electrochemical atomic layer deposition (E-ALD): studies using voltammetry and in situ scanning tunneling microscopy. *The Journal of Physical Chemistry C* **2013**, *117*, 15728-15740.

(31) Lukaszewski, M.; Hubkowska, K.; Czerwinski, A. Electrochemical absorption and oxidation of hydrogen on palladium alloys with platinum, gold and rhodium. *Physical Chemistry Chemical Physics* **2010**, *12*, 14567-14572.

(32) Żurowski, A.; Łukaszewski, M.; Czerwiński, A. Electrosorption of hydrogen into palladium–rhodium alloys. *Electrochimica Acta* **2006**, *51*, 3112-3117.

(33) Sheridan, L. B.; Yates, V. M.; Benson, D. M.; Stickney, J. L.; Robinson, D. B. Hydrogen sorption properties of bare and Rh-modified Pd nanofilms grown via surface limited redox replacement reactions. *Electrochimica Acta* **2014**, *128*, 400-405.

(34) Brenner, A.; Riddell, G. E. Nickel Plating on Steel by Chemical Reduction. *Journal of Research of the National Bureau of Standards* **1946**, *37*, 31-34.

(35) Cappillino, P. J.; Sugar, J. D.; El Gabaly, F.; Cai, T. Y.; Liu, Z.; Stickney, J. L.; Robinson, D. B. Atomic-Layer Electroless Deposition: A Scalable Approach to Surface-Modified Metal Powders. *Langmuir* **2014**.

(36) Nutariya, J.; Fayette, M.; Dimitrov, N.; Vasiljevic, N. Growth of Pt by surface limited redox replacement of underpotentially deposited hydrogen. *Electrochimica Acta* **2013**, *112*, 813-823.

(37) Ambrozik, S.; Dimitrov, N. The Deposition of Pt via Electroless Surface Limited Redox Replacement. *Electrochimica Acta* **2015**, *169*, 248-255.

(38) Ambrozik, S.; Rawlings, B.; Vasiljevic, N.; Dimitrov, N. Metal deposition via electroless surface limited redox replacement. *Electrochemistry Communications* **2014**, *44*, 19-22.

(39) Mallory, G. O.: The Fundamental Aspects of Electroless Nickel Plating. In *Electroless Plating: Fundamentals and Applications*; Mallory, G. O., Hajdu, J.B., Ed.; Noyes Publications/William Andrew Publishing, LLC: Norwich, NY, 1990.

(40) Sudagar, J.; Lian, J.; Sha, W. Electroless nickel, alloy, composite and nano coatings – A critical review. *Journal of Alloys and Compounds* **2013**, *571*, 183-204.

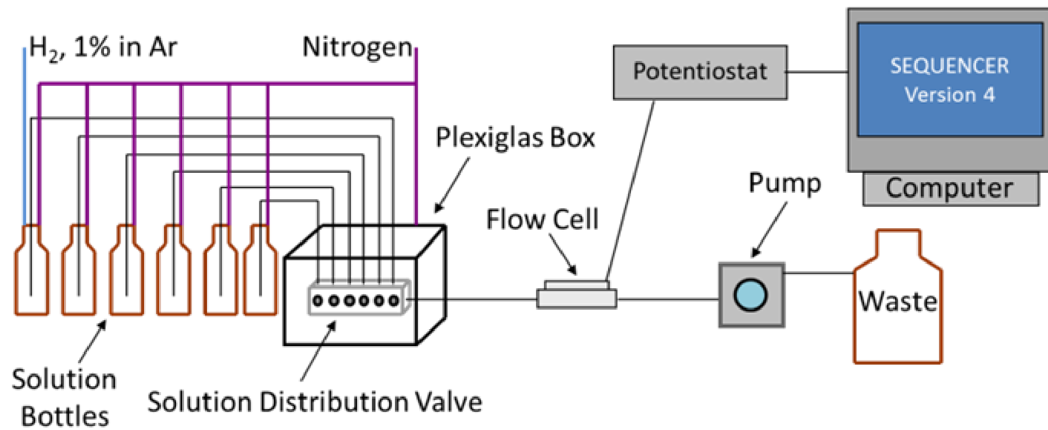

Figure 1.1: Schematic of the flow cell system used.

CHAPTER 2

ENHANCED KINETICS OF ELECTROCHEMICAL HYDROGEN UPTAKE AND RELEASE ON PALLADIUM POWDERS MODIFIED BY ELECTROCHEMICAL ATOMIC LAYER DEPOSITION[1]

[1] D. Benson, C. Tsang, J. Sugar, K. Jagannathan, D. Robinson, F. El Gabaly, P. Cappillino, and J. Stickney, To be submitted to *ACS Materials and Interfaces (2015)*

Abstract

Electrochemical atomic layer deposition (E-ALD) is a method for the formation of nanofilms of materials, an atomic layer at a time. It uses the galvanic exchange of a less noble metal, deposited by underpotential deposition (UPD), to produce an atomic layer of a more noble element by reduction of its ions. This process is referred to as surface limited redox replacement (SLRR), and can be repeated in a cycle to grow thicker deposits. It was previously performed on nanoparticles and planar substrates. In the present report, E-ALD has been applied to coating a sub-micron sized powder substrate, making use of a new flow cell design. E-ALD was used to coat a Pd powder with different thicknesses of Rh or Pt by exchanging it for Cu UPD. Scanning transmission electron microscopy with energy dispersive X-ray spectroscopy showed conformal deposition across all surface features. Cyclic voltammetry and X-ray photoelectron spectroscopy indicated an increasing Rh coverage with increasing numbers of deposition cycles performed, in a manner consistent with an ALD mechanism. Cyclic voltammetry also indicated increased kinetics of H sorption and desorption into and out of the Pd powder with the Rh present, relative to unmodified Pd.

Introduction

Atomic layer deposition (ALD) makes use of surface limited reactions in a cycle, to form nanofilms conformally on a substrate.[1] The result is material formation one atomic layer at a time, where an atomic layer is no more than one atom in thickness. ALD is generally performed in a gas or vacuum phase reactor, and has been remarkably successful in forming oxide nanofilms.[2,3]

Electrochemical atomic layer deposition (E-ALD) is a condensed phase version of ALD, based on the use of underpotential deposition (UPD), [4-6] an electrochemical form of surface limited reaction.[7-9] UPD results from the favorable free energy of formation of a compound or alloy and involves the deposition of one element on a second at a potential prior to ("under", generally meaning more positive than) that needed to deposit the element on itself. UPD generally results in the deposition of an atomic layer, with a maximum coverage of about one monolayer (ML), defined in this report as one adsorbate atom per substrate surface atom. E-ALD cycles consisting of surface limited redox replacement (SLRR) were employed to deposit Rh. SLRR involves first depositing an atomic layer of a sacrificial metal by UPD, which should be less noble than the metal to be deposited.[10-14] The solution is then exchanged, at open circuit, for one containing an ionic precursor for the desired element. The depositing element is reduced using electrons from the sacrificial UPD layer, the coverage of which accounts for limiting the amount of the desired element formed. Rinsing with blank completes the SLRR cycle, which can be repeated to form thicker deposits.[15-17] E-ALD has been used in the present study because of the control it offers over Rh nanofilm deposit coverages. SLRR on nanoparticles was previously demonstrated by Pt deposition on Au nanoparticles for oxygen reduction.[18]

Studies of E-ALD have, thus far, primarily involved deposition on flat surfaces,[19-22] except for studies using SLRR, which was initially developed in order to coat the surfaces of nanoparticles with minimum quantities of catalytic metals.[11,23] Previous work has shown that modification of the surface of a Pd nanofilm with Rh resulted in enhanced rates for H absorption and desorption.[24] That study involved deposits formed on flat Au

on glass substrates. The present studies were undertaken to investigate similar deposits on the surfaces of three-dimensional materials, in the form of submicron-sized powders. Such powders have applications in hydrogen separations, fuel cells, sensors, and catalysts.[25-28] Prior work on hydrogen reactions with powders has involved both elemental and alloy powders.[29-31] Powders typically allow for a much larger electrochemical surface area, for a given superficial surface area, compared to a planar substrate, increasing the rates of interfacial reactions.[32] Powders have been studied as media for storage or separation of bulk amounts of hydrogen.[33,34]

Two of the mechanisms for H absorption proposed in the literature are direct and indirect absorption. In the direct absorption mechanism, hydrogen is absorbed by Pd in one step, where $H_3O^+ + e^- \rightarrow H_{abs} + H_2O$.[35] The indirect mechanism suggests that hydrogen first forms a surface hydride prior to moving into empty subsurface sites, then finally diffuses into the bulk Pd.[32,36] Recent publications theorize that modification of Pd surfaces with submonolayer amounts of another element may destabilize the surface hydride, allowing an increase in the rate for adsorbed hydrogen being transferred from the surface into the bulk.[35,37] Reports in the literature supporting that theory suggest that Pd powders with a surface modified by Rh or Pt enhance both hydrogen absorption and desorption.[38] This report investigates the effect of Pd surface modification with SLRR Rh on the rates of hydrogen absorption and desorption, to ask whether the effect seen on films also applies to the more complex geometries and surface microstructures of powders.[39,40] If so, it would suggest that the indirect mechanism is relevant in this case.

In the present study, hardware and methodologies for surface modification using E-ALD of Rh and Pt on high surface area powders were investigated. Typical powder

samples, such as those considered here, have much larger electrochemically active surface areas per unit volume compared with planar films. Use of E-ALD to modify powders will result in a much greater yield of modified surface area than it would on planar substrates, but requires certain considerations to ensure that reactions can proceed uniformly and completely.

Experimental Methods

All solutions were prepared using 18 MΩ cm water from a water filtration system (Milli-Q Advantage A10). The Rh solution contained 0.1 mM $RhCl_3$ (Sigma-Aldrich, 99.9%, trace metals basis) in 0.1 M H_2SO_4 (Fisher, analytical grade). Pt solution was 0.1 mM H_2PtCl_6 (Fisher, ultrapure grade) with 50 mM $HClO_4$ (J.T. Baker, A.C.S. reagent grade). The sacrificial metal solution was 2 mM $CuSO_4$ (J.T. Baker, 99.8%) in 0.1 M H_2SO_4. The blank solution was 0.1 M H_2SO_4. During use, and for at least 60 minutes prior, all solutions were degassed with N_2 to remove dissolved O_2.

E-ALD experiments were performed using an automated flow cell system (Electrochemical ALD, L.C.) consisting of a variable speed pump, solenoid selection valve, solution reservoirs, potentiostat (PARR), and a three electrode flow cell. Sequencer 4.0 control software (Electrochemical ALD, L.C.) was used to form the deposits. The flow cell (Figure 2.1) was designed to hold powdered substrates and allowed solution exchange while under potential control. The design consisted of two sides, each with flat silica frits. The sample was placed between the frits, inside of two pieces of nitrocellulose filter paper (Millipore, 0.45 μm). Two rubber gasket rings were placed around the substrate and prevented leaking at the joint. Electrical contact was made using a piece of Teflon-coated Pt wire (Med Wire), where the stripped end was

placed inside the Pd powder substrate, and the Teflon-coated region passed between the two gaskets. The entire ensemble was held together with a metal clamp. A Pt mesh cage (diameter 0.5”, length 2”) served as the auxiliary electrode and was housed in the upper column. A reference electrode compartment, containing an Ag/AgCl (3 M KCl) electrode (Bioanalytical Systems, Inc.), was located at the ingress to the cell. All potentials were reported vs. the Ag/AgCl reference. Solutions were drawn from reservoirs, through a valve block, and then pumped past the reference and through the powdered working electrode. After the working electrode, the solutions entered the auxiliary electrode compartment, from which they were pumped to waste, along with any gaseous products produced at the auxiliary electrode. All cyclic voltammograms were collected at a scan rate of 10 mV/s in 0.1 M H_2SO_4.

In each experiment, 50 to 300 mg of Pd powder (Sandia National Laboratories Powder Metallurgical Facility) was placed in the flow cell and soaked in 0.1 M H_2SO_4 for approximately 30 minutes to ensure uniform wetting of the membranes and the powder, promoting uniform solution flow, and ensuring complete electrical connection. A voltammetric cleaning method similar to that used for planar Au[41] substrates was applied to clean the Pd powder, though the upper potential limit was decreased from 1.4 V to 1.2 V to avoid oxygen evolution. After cycling the potential between -0.2 V and +1.2 V in 0.1 M H_2SO_4 to clean the Pd surface, the potential cycling was stopped at 0.15 V and held, prior to the experiment.

The procedure for Rh deposition by E-ALD is illustrated in Figure 2.2. A typical cycle involved first flowing the Cu^{2+} ion solution into the cell at a rate of 2 mL/min with the potential held at 0.15 V, until the solution was at equilibrium with the substrate,

indicated by the absence of Cu deposition current. The potential was then allowed to go to open circuit, and Rh solution was flowed through the cell. The Rh^{3+} solution was pumped through the cell until the potential increased to 0.39 V, a pre-determined “stop” potential, in order to avoid Pd oxidation. Reaching the stop potential is assumed to indicate that the Cu UPD atomic layer had been completely exchanged for 2/3 as many atoms of Rh, based on the expected stoichiometry. In the final step of the cycle, the Rh^{3+} solution was rinsed out with blank solution. Thicker Rh films were deposited by repeating this cycle on the Pd substrate the desired number of times. Deposits were performed where the Rh SLRR cycle was repeated 1, 3, 6, and 20 times on Pd powders. The same deposition method was applied using Pt^{4+} solution in place of the Rh^{3+} to create Pt deposits on Pd powder. After deposition the samples were rinsed with purified water and dried under vacuum.

Studies of the kinetics for hydrogen absorption and desorption were performed with much smaller quantities of Pd powder, using a different flow cell configuration due to mass transport limitations that become important on fast timescales. This approach used a glassy carbon electrode, a GLAS-10 grade 1 cm^2 substrate (SPI Supplies), which had an exposed surface area of 0.71 cm^3, defined by Poly Donut masking tape (EPSI).

The studies of kinetics were performed in a standard E-ALD flow cell, with a few mg of Pd powder. [42] To hold the small amounts of powder, the procedure shown in Figure 2.3 was developed. To prepare the sample, a well was created using tape with a hole of the desired size punched in the center. This was applied to the Au slide surface. The Au served as a contact for the Pd powder working electrode. The powder was placed on the exposed Au, then covered with a piece of nitrocellulose membrane filter, which

was held down with a piece of double sided tape. This sample was then placed in the flow cell on a 1.5 mm thick gasket (defining the solution volume) to perform electrochemical experiments. It was found, however, that the fragility of the nitrocellulose membrane often caused it to tear or rupture, allowing some powder to escape, thereby introducing inconsistency in mass from one sample to the next. Additionally, some Pd was observed to strongly bond or alloy with the Au, forming dark areas on the Au surface.

In order to maintain greater control and reproducibility with small quantities of Pd powder, a different containment method was implemented where 1 mg sample of Pd powder was studied by pressing it into the glassy C electrode surface prior to inserting it into the cell.[42] This sample was then placed in the flow cell on a 1.5 mm thick gasket to perform electrochemical experiments.

Scanning electron microscopy (SEM) was performed using an FEI Inspect F system at 20 kV. X-ray photoelectron spectroscopy (XPS) data was obtained at the Advanced Light Source at Lawrence Berkeley National Laboratory (XPS endstation at beam line 9.3.2)[43] and a laboratory spectrometer with an Omicron DAR400 Al K-alpha X-ray source and Physical Electronics 10-360 electron energy analyzer. Further details are available in previously published work by Cappillino, et al.[38]

The compositional distribution of PdRh powder particles was imaged by scanning transmission electron microscopy (STEM). Following published literature[44,45], the particles were mounted in epoxy (Struers), then sectioned using a diamond knife with a Leica EM UC6 ultramicrotome. The resulting electron-transparent samples were subjected to compositional analysis using a probe-corrected FEI Titan G2 80-200 with a large-area silicon drift EDS (energy dispersive X-ray spectroscopy) detector

(ChemiSTEM). Individual EDS spectra were acquired at every image pixel for the EDS spectrum images. The Cliff-Lorimer *k* factor method was applied for quantitative compositional analysis.[46] The *k* factor was obtained from measurements of a known reference material (8 at. % Rh-Pd), the composition of which was verified by X-ray fluorescence.

Results

An estimate of the surface area expected for a given powder mass of particles is described using Table 2.1. The estimate assumed the powder particles were spherical with a diameter of approximately 1 μm. A mass of 50 mg was used in the initial calculation. Using the density of Pd, and both the volume and surface area for a sphere, estimates were made of the volume a given mass of powder should occupy, how many particles would be present, and the corresponding surface area. For a 50 mg sample of Pd powder, the surface area was estimated to be 250 cm^2, or 0.5 m^2/g of Pd powder, comparable to the measured 0.4 m^2/g, noted below.

Scanning electron microscope (SEM) images indicated the particles were between 0.2 and 0.4 μm (Figure 2.4). As expected, the Pd powder exhibited much higher currents than Pd films with an equivalent cross section, due to their greatly increased surface areas. Cyclic voltammograms were performed on 50 mg (black) and 300 mg samples of bare Pd powder (Figure 2.5, top). Starting at open circuit potential around 300 mV, the potential was scanned to -0.25 V. Hydrogen adsorption peaks begin just positive of 0 V, and the absorption peak begins at -0.1 V in the black plot for the 50 mg sample, but initially overlaps with the adsorption peak in the red plot for the 300 mg sample. The scan was reversed at -0.25 V. Hydrogen desorption was evidenced by the rapid increase

in current, which decays and nears 0 mA around 0.1 V. Pd oxidation features are seen during the positive scan starting at about 0.35 V and continuing until the scan was reversed at 1.2 V. Surface areas were measured by integration of the Pd oxide reduction peak[47] at 400 mV, and found to be proportional to the mass of powder (Figure 2.5, bottom). This suggests that the surface areas were equally accessed by solution. Comparing the charges for oxide reduction of SLRR Pd on Au and of powder samples to a PVD Pd film on a Si wafer allowed an estimate of the surface area per unit mass of powder: 0.4 m^2/g (Table 2.2).

Potential and current-time traces for Cu deposition on Pd powder for Rh exchange are shown in Figure 2.6. For this 300 mg Pd powder sample, a maximum of approximately 20 mA of current is observed. About 2 minutes was the time required to completely deposit the Cu, as indicated by the current returning to zero.

During SLRR on powder, it was observed that the time required for Rh to exchange with the Cu UPD increased with each cycle, as did the subsequent cycle's charge for Cu UPD (Figure 2.7). Those results suggest an increase in surface area, possibly due to Volmer-Weber growth of Rh on the Pd particles, though it may also indicate an increase in wetted surface area.

Cyclic Voltammetry (CV) of coated samples

CV was performed on Pd powder samples coated with Rh, using the powder flow cell (Figure 2.1), to compare with uncoated Pd powder (Figure 2.8). The loss of Pd surface hydride peak area around 0 V indicates that the Rh is covering the Pd surface, preventing H adsorption. No kinetic enhancements in the rate of hydrogen absorption or desorption were observed from the CVs. This can be concluded because the CV profiles

for proton reduction and hydrogen oxidation were essentially the same before and after the Rh SLRR cycles. It is possible that, in both of these CVs, current is limited by mass transport effects and solution resistance rather than surface kinetics. CVs using smaller quantities of powder can be expected to allow more rapid transport into the interior of a powder mass, and might yield observable kinetic effects, such as those previously shown on planar substrates,[38] so we have performed these experiments.

CVs of a powdered sample pressed into glassy carbon were run both prior to and following three Rh SLRR cycles (Figure 2.9). As with Rh deposition on Pd films, the Pd surface hydride peaks at -0.05 V were diminished, indicating partial coverage of the surface by Rh, while the H absorption and desorption peaks showed higher currents that occurred earlier in the potential cycle. This demonstrates that, on a 1 mg sample, H sorption kinetics were faster when the surface was modified with Rh.

Scanning Transmission Electron Microscopy with Energy Dispersive X-ray Spectroscopy (STEM-EDS)

Figure 2.10 (middle row) shows an overlay map of rhodium and palladium STEM-EDS signals for epoxy-embedded, microtomed Pd powder samples on which one and six SLRR cycles for Rh had been performed. In both cases there is an elevated Rh signal that follows the contour of the surface of the particle, including concave regions. The thickness was uniform to within a few nanometers in each case. Large bare regions with no rhodium are not observed here. It is apparent that the rhodium was not depositing as isolated islands on the length scale of these particles, but was instead forming a uniform layer to within the resolution of the instrument, which approaches

atomic dimensions. The quantity of rhodium at the interface for the 6x case is higher than the 1x case, but not by a factor of 6.

X-Ray photoelectron spectroscopy (XPS)

XPS is complementary to STEM-EDS, because it provides surface-specific information from a much larger volume of sample. Lower incident photon energies have lower escape depths, so measuring spectra at several photon energies provides greater detail concerning the surface structure than measurement at a single photon energy. Pd powder samples on which 1, 3, and 6 Rh cycles had been performed were measured using 450 and 850 eV synchrotron photons, as well as using 1487 eV photons obtained on a laboratory instrument. The NIST software package SESSA was used to compute simulated spectra for a bare Pd film and an 8 nm Rh film (essentially an infinitely thick Rh sample), and a 0.24 nm Rh layer on Pd, representing approximately one atomic layer.[48] Linear combinations of those spectra were compared with the experimental data to determine the best fit. The experimental and simulated spectra were background corrected and integrated in CasaXPS software using the Shirley method.[49]

Figure 2.11 displays experimental and best-fit simulated data for one, three, and six cycles of Rh deposited on Pd. The amount of Rh increased with the number of cycles for both the simulations and experiments. The differences between the 450 eV spectra and those at higher incident energy were larger than the differences between 850 and 1487 eV, especially for the thicker films. This is due to the significantly lower electron escape depth for the 450 eV spectra.

The simulations (Figure 2.12) suggest that the 1 cycle sample surface consisted of a mix of about 80% bare Pd and 20% thin Rh, and the 3 cycle sample showed only

slightly more thin Rh. It is interesting to note that gas-phase ALD of Pd on alumina was reported to produce only about 20% coverage after 200 cycles.[50] The 6 cycle sample, however, showed a significantly larger fraction of Rh, and required ~2% coverage of thick Rh to obtain a best fit. While the STEM-EDS images suggest that the layers are uniform and conformal on the scale of tens of nanometers, the XPS analysis suggests that some nonuniformity is present at different length scales. The average Rh thickness is primarily in the submonolayer regime for the few cycles performed in this study. If much three-dimensional growth had been occurring, the fits to the XPS experiments would have appeared more like that of the 8.0 nm Rh simulation, and we would expect to see larger islands or dendrites in the STEM images. The simulated amounts of bare Pd are qualitatively consistent with the results from cyclic voltammetry, which showed a decreasing Pd surface hydride peak with increasing thickness, though some Pd surface hydride was still formed after 3-cycles of Rh deposition.

Platinum deposited on Pd

Platinum deposits that were created using the same deposition sequence parameters as the Rh samples were examined using STEM-EDS (Figure 2.13). High-angle annular dark field spectroscopy is shown in the left column, with highlighted boxes depicting the areas enlarged in the right column as a Pt (red) on Pd (green) overlay map. The images zoom in on the same particle moving downward through the figure. Similar to the results for Rh deposition, the Pt is shown to cover the Pd particle surface regardless of morphology without significant gaps in coverage or variance in thickness.

XPS data indicates increasing Pt signal for both the $4f_{3/2}$ (69 eV) and $4f_{5/2}$ (72.5 eV) peaks with increased Pt deposition cycles (Figure 2.14, top). The image was

processed using CASA software for background subtraction, and Origin software to complete a 4 point Savitzky-Golay smoothing routine. Data collected using an excitation energy of 850 eV for samples of 1, 3, and 6 cycles of Pt SLRR on Pd powder are shown in black, red, and blue, respectively. The Pt 4f peak heights and areas increase with subsequent deposition cycles while the Pd 3d peaks decrease (Figure 2.13, bottom), consistent with increasing surface coverage with increasing deposition. A table of both Rh 3d peak area and Pt 4f peak area vs the number of Rh and Pd SLRR deposition cycles, respectively, (Table 2.3) was created with the Rh 3d and Pt 4f peak areas normalized to the Pd 3d peak area. At all excitation energies, the peak area for deposited Pt increases with increasing number of deposition cycles. This same trend is observed for the deposition of Rh. For each deposited metal, Rh and Pt, the peak areas are largest for data collected at the excitation energy of 450 eV and smallest for the data collected at 850 eV. The decrease in peak area with increasing excitation energy corresponds with the deposit remaining on top of the Pd surface, as higher energy X-rays penetrate more deeply, giving larger peaks for the internal Pd, and smaller peaks for the elements deposited on the surface: Rh and Pt. The XPS plots and the peak area values in the table both indicate that the Rh and Pt thickness does increase with increasing deposition cycles, and it appears to do so with an increased rate as cycles continue. These data indicate that SLRR has been successfully applied to a powder substrate.

Conclusion and outlook

The use of E-ALD to grow Rh and Pt nanofilms on a powdered electrode has been demonstrated. The rates of hydrogen absorption and desorption by Pd powder increased after monolayer-scale amounts of Rh were deposited, as observed using cyclic

voltammetry. The voltammetry also indicated the presence of Rh on the surface by a decrease of the Pd surface hydride peaks. XPS analysis showed evidence of monolayer-scale Rh and Pt present on the surface, which increased with the number of cycles. STEM-EDS elemental mapping showed Rh and Pt confined to the outer surface of the Pd particles, in a uniform, conformal coating on the nanometer length scale. The enhanced H absorption and desorption kinetics support an indirect mechanism for H transport, occurring via a surface hydride intermediate. The presence of Rh appears to affect that intermediate. Pt kinetics on powder have not yet been examined.

This report suggests that the broad range of cycle chemistries accessible to the E-ALD method[51,52] are applicable to powdered conductive substrates. Scale up to larger quantities of powder may require a larger flow cell and counter electrode, and potentiostat that can deliver adequate current. The presented experiments produced approximately 50 μA of current per mg of powder during Cu deposition, and the current can be expected to scale with the mass of the batch, assuming constant particle size, although mass transport limitations and solution resistance may result in lower currents and longer cycle times. A similar and potentially more scalable deposition method, atomic layer electroless deposition (ALED), has recently been developed.[38] This method applies a similar method to SLRR, except it uses hydrogen adsorbed or dilutely absorbed at open circuit to act as a sacrificial element to allow a metal such as Rh to exchange and form a deposit on the metal surface.[53] While ALED is less likely to suffer from such scaling limitations, its versatility is limited by the number of substrates that can form surface hydrides. E-ALD has been demonstrated to form deposits in other potential ranges, not only where hydrides form. This work has helped establish that E-ALD is

versatile not only in the materials that can be deposited, but also in the substrates that can be used.

Acknowledgments

Acknowledgment is made of the support of the National Science Foundation, Division of Materials Research #1410109, as well as the Laboratory-Directed Research and Development program at Sandia National Laboratories, a multi-program laboratory managed and operated by Sandia Corporation, a wholly owned subsidiary of Lockheed Martin Corporation, for the U.S. Department of Energy's National Nuclear Security Administration under contract DE-AC04-94AL85000. XPS data was obtained at the Advanced Light Source at Lawrence Berkeley National Laboratory (XPS endstation at beam line 9.3.2; Zhi Liu, beamline scientist), supported by the Director, Office of Science, Office of Basic Energy Sciences, of the U.S. Department of Energy under Contract No. DE-AC02-05CH11231.

References

(1) George, S. M. Atomic Layer Deposition: An Overview. *Chemical Reviews* **2009**, *110*, 111-131.

(2) Christensen, S. T.; Feng, H.; Libera, J. L.; Guo, N.; Miller, J. T.; Stair, P. C.; Elam, J. W. Supported Ru−Pt Bimetallic Nanoparticle Catalysts Prepared by Atomic Layer Deposition. *Nano Letters* **2010**, *10*, 3047-3051.

(3) Lu, J.; Low, K.-B.; Lei, Y.; Libera, J. A.; Nicholls, A.; Stair, P. C.; Elam, J. W. Toward atomically-precise synthesis of supported bimetallic nanoparticles using atomic layer deposition. *Nat Commun* **2014**, *5*.

(4) Adzic, R. R.: Electrocatalytic Properties of the Surfaces Modified by Foreign Metal Adatoms. Wiley-Interscience: New York, 1984.

(5) Kolb, D. M.: Advances in Electrochemistry and Electrochemical Engineering. John Wiley: New York, 1978.

(6) Magnussen, O. M. Ordered Anion Adlayers on Metal Electrode Surfaces. *Chemical Reviews* **2002**, *102*, 679-726.

(7) Gregory, B. W.; Norton, M. L.; Stickney, J. L. Thin-layer electrochemical studies of the underpotential deposition of cadmium and tellurium on polycrystalline Au, Pt and Cu electrodes. *Journal of Electroanalytical Chemistry* **1990**, *293*, 85-101.

(8) Gregory, B. W.; Stickney, J. L. Electrochemical atomic layer epitaxy (ECALE). *Journal of Electroanalytical Chemistry* **1991**, *300*, 543-561.

(9) Gregory, B. W.; Suggs, D. W.; Stickney, J. L. Conditions for the Deposition of CdTe by Electrochemical Atomic Layer Epitaxy. *Journal of The Electrochemical Society* **1991**, *138*, 1279-1284.

(10) Herrero, E.; Buller, L. J.; Abruña, H. D. Underpotential Deposition at Single Crystal Surfaces of Au, Pt, Ag and Other Materials. *Chemical Reviews* **2001**, *101*, 1897-1930.

(11) Brankovic, S. R.; Wang, J. X.; Adžić, R. R. Metal monolayer deposition by replacement of metal adlayers on electrode surfaces. *Surface Science* **2001**, *474*, L173-L179.

(12) Mrozek, M. F.; Xie, Y.; Weaver, M. J. Surface-enhanced Raman scattering on uniform platinum-group overlayers: preparation by redox replacement of underpotential-deposited metals on gold. *Analytical chemistry* **2001**, *73*, 5953-5960.

(13) Kim, Y.-G.; Kim, J. Y.; Vairavapandian, D.; Stickney, J. L. Platinum Nanofilm Formation by EC-ALE via Redox Replacement of UPD Copper: Studies Using in-Situ Scanning Tunneling Microscopy. *The Journal of Physical Chemistry B* **2006**, *110*, 17998-18006.

(14) Vasilic, R.; Dimitrov, N. Epitaxial Growth by Monolayer-Restricted Galvanic Displacement. *Electrochemical and Solid-State Letters* **2005**, *8*, C173-C176.

(15) Jayaraju, N.; Vairavapandian, D.; Kim, Y. G.; Banga, D.; Stickney, J. L. Electrochemical Atomic Layer Deposition (E-ALD) of Pt Nanofilms Using SLRR Cycles. *Journal of The Electrochemical Society* **2012**, *159*, D616-D622.

(16) Sheridan, L. B.; Gebregziabiher, D. K.; Stickney, J. L.; Robinson, D. B. Formation of Palladium Nanofilms Using Electrochemical Atomic Layer Deposition (E-ALD) with Chloride Complexation. *Langmuir* **2013**, *29*, 1592-1600.

(17) Thambidurai, C.; Kim, Y.-G.; Stickney, J. L. Electrodeposition of Ru by atomic layer deposition (ALD). *Electrochimica Acta* **2008**, *53*, 6157-6164.

(18) Loukrakpam, R.; Yuan, Q.; Petkov, V.; Gan, L.; Rudi, S.; Yang, R.; Huang, Y.; Brankovic, S. R.; Strasser, P. Efficient C-C bond splitting on Pt monolayer and sub-monolayer catalysts during ethanol electro-oxidation: Pt layer strain and morphology effects. *Physical Chemistry Chemical Physics* **2014**, *16*, 18866-18876.

(19) Lin, S. X.; Shi, X. Z.; Zhang, X.; Kou, H. H.; Wang, C. M. Ternary semiconductor compounds CuInS2 (CIS) thin films synthesized by electrochemical atomic layer deposition (EC-ALD). *Applied Surface Science* **2010**, *256*, 4365-4369.

(20) Innocenti, M.; Becucci, L.; Bencista, I.; Carretti, E.; Cinotti, S.; Dei, L.; Benedetto, F. D.; Lavacchi, A.; Marinelli, F.; Salvietti, E.; Vizza, F.; Foresti, M. L. Electrochemical growth of Cu-Zn sulfides. *Journal of Electroanalytical Chemistry* **2013**, *710*, 17-21.

(21) Valdes, M.; Modibedi, M.; Mathe, M.; Hillie, T.; Vazquez, M. Electrodeposited Cu2ZnSnS4 thin films. *Electrochimica Acta* **2014**, *128*, 393-399.

(22) Zhang, L.; He, W. Y.; Chen, X. Y.; Du, Y.; Zhang, X.; Shen, Y. H.; Yang, F. C. Nanocrystallized Cu2Se grown on electroless Cu coated p-type Si using electrochemical atomic layer deposition. *Surface Science* **2015**, *631*, 173-177.

(23) Brankovic, S. R.; Wang, J. X.; Adžić, R. R. Pt Submonolayers on Ru Nanoparticles: A Novel Low Pt Loading, High CO Tolerance Fuel Cell Electrocatalyst. *Electrochemical and Solid-State Letters* **2001**, *4*, A217-A220.

(24) Sheridan, L. B.; Yates, V. M.; Benson, D. M.; Stickney, J. L.; Robinson, D. B. Hydrogen sorption properties of bare and Rh-modified Pd nanofilms grown via surface limited redox replacement reactions. *Electrochimica Acta* **2014**, *128*, 400-405.

(25) Li, M.; Yang, W. F. Highly porous palladium bulk: Preparation and properties as active metal material for displacement chromatographic process. *Int. J. Hydrog. Energy* **2009**, *34*, 1585-1589.

(26) Antolini, E. Palladium in fuel cell catalysis. *Energy & Environmental Science* **2009**, *2*, 915-931.

(27) Leparmentier, S.; Auguste, J. L.; Humbert, G.; Delaizir, G.; Delepine-Lesoille, S.; Bertrand, J.; Buschaert, S.; Perisse, J.; Mace, J. R. Palladium particles embedded into silica optical fibers for hydrogen gas detection. *Proceedings of SPIE* **2014**, *9128*, 9.

(28) Shao, M. Palladium-based electrocatalysts for hydrogen oxidation and oxygen reduction reactions. *Journal of Power Sources* **2011**, *196*, 2433-2444.

(29) Fazle Kibria, A. K. M.; Sakamoto, Y. The effect of alloying of palladium with silver and rhodium on the hydrogen solubility, miscibility gap and hysteresis. *Int. J. Hydrog. Energy* **2000**, *25*, 853-859.

(30) Lototsky, M. V.; Williams, M.; Yartys, V. A.; Klochko, Y. V.; Linkov, V. M. Surface-modified advanced hydrogen storage alloys for hydrogen separation and purification. *Journal of Alloys and Compounds* **2011**, *509, Supplement 2*, S555-S561.

(31) Mallát, T.; Polyánszky, É.; Petró, J. Electrochemical study of palladium powder catalysts. *Journal of Catalysis* **1976**, *44*, 345-351.

(32) Ward, T. L.; Dao, T. Model of hydrogen permeation behavior in palladium membranes. *Journal of Membrane Science* **1999**, *153*, 211-231.

(33) Foltz, G. W.; Melius, C. F. Studies of isotopic exchange between gaseous hydrogen and palladium hydride powder. *Journal of Catalysis* **1987**, *108*, 409-425.

(34) Heung, L. K.; Sessions, H. T.; Xiao, X. TCAP Hydrogen Isotope Separation Using Palladium and Inverse Columns. *Fusion science and technology* **2011**, *60*, 1331-1334.

(35) Bartlett, P. N.; Marwan, J. The effect of surface species on the rate of H sorption into nanostructured Pd. *Physical Chemistry Chemical Physics* **2004**, *6*, 2895-2898.

(36) Jerkiewicz, G.; Zolfaghari, A. Comparison of Hydrogen Electroadsorption from the Electrolyte with Hydrogen Adsorption from the Gas Phase. *Journal of The Electrochemical Society* **1996**, *143*, 1240-1248.

(37) Greeley, J.; Mavrikakis, M. Surface and Subsurface Hydrogen: Adsorption Properties on Transition Metals and Near-Surface Alloys. *The Journal of Physical Chemistry B* **2005**, *109*, 3460-3471.

(38) Cappillino, P. J.; Sugar, J. D.; El Gabaly, F.; Cai, T. Y.; Liu, Z.; Stickney, J. L.; Robinson, D. B. Atomic-Layer Electroless Deposition: A Scalable Approach to Surface-Modified Metal Powders. *Langmuir* **2014**.

(39) Lukaszewski, M.; Hubkowska, K.; Czerwinski, A. Electrochemical absorption and oxidation of hydrogen on palladium alloys with platinum, gold and rhodium. *Physical Chemistry Chemical Physics* **2010**, *12*, 14567-14572.

(40) Żurowski, A.; Łukaszewski, M.; Czerwiński, A. Electrosorption of hydrogen into palladium–rhodium alloys. *Electrochimica Acta* **2006**, *51*, 3112-3117.

(41) Sheridan, L. B.; Czerwiniski, J.; Jayaraju, N.; Gebregziabiher, D. K.; Stickney, J. L.; Robinson, D. B.; Soriaga, M. P. Electrochemical atomic layer deposition

(E-ALD) of palladium nanofilms by surface limited redox replacement (SLRR), with EDTA complexation. *Electrocatalysis* **2012**, *3*, 96-107.

(42) Flowers Jr, B. H.; Wade, T. L.; Garvey, J. W.; Lay, M.; Happek, U.; Stickney, J. L. Atomic layer epitaxy of CdTe using an automated electrochemical thin-layer flow deposition reactor. *Journal of Electroanalytical Chemistry* **2002**, *524–525*, 273-285.

(43) Grass, M. E.; Karlsson, P. G.; Aksoy, F.; Lundqvist, M.; Wannberg, B.; Mun, B. S.; Hussain, Z.; Liu, Z. New ambient pressure photoemission endstation at Advanced Light Source beamline 9.3.2. *Review of Scientific Instruments* **2010**, *81*, 053106.

(44) Johnson, P. B.; Thomson, R. W.; Reader, K. TEM and SEM studies of radiation blistering in helium-implanted copper. *Journal of Nuclear Materials* **1999**, *273*, 117-129.

(45) Hochella Jr, M. F.; Moore, J. N.; Golla, U.; Putnis, A. A TEM study of samples from acid mine drainage systems: metal-mineral association with implications for transport. *Geochimica et Cosmochimica Acta* **1999**, *63*, 3395-3406.

(46) Cliff, G. L., G.W. The quantitative analysis of thin specimens. *J. Microsc. (Oxford)* **1975**, *103*, 203-207.

(47) Rand, D. A. J.; Woods, R. A study of the dissolution of platinum, palladium, rhodium and gold electrodes in 1 m sulphuric acid by cyclic voltammetry. *Journal of Electroanalytical Chemistry and Interfacial Electrochemistry* **1972**, *35*, 209-218.

(48) Smekal, W.; Werner, W. S. M.; Powell, C. J. Simulation of electron spectra for surface analysis (SESSA): a novel software tool for quantitative Auger-electron spectroscopy and X-ray photoelectron spectroscopy. *Surface and Interface Analysis* **2005**, *37*, 1059-1067.

(49) Fairley, N.: *CasaXPS manual 2.3. 15*; Acolyte Science, 2009.

(50) Weber, M. J.; Mackus, A. J. M.; Verheijen, M. A.; Longo, V.; Bol, A. A.; Kessels, W. M. M. Atomic Layer Deposition of High-Purity Palladium Films from Pd(hfac)2 and H2 and O2 Plasmas. *The Journal of Physical Chemistry C* **2014**, *118*, 8702-8711.

(51) Stickney, J. L.: Electrochemical atomic layer epitaxy. I. Rubenstein, A. J. B., Ed.; Marcel Dekker: New York, 1999; pp 75-209.

(52) Switzer, J. A. Atomic Layer Electrodeposition. *Science* **2012**, *338*, 1300-1301.

(53) Nutariya, J.; Fayette, M.; Dimitrov, N.; Vasiljevic, N. Growth of Pt by surface limited redox replacement of underpotentially deposited hydrogen. *Electrochimica Acta* **2013**, *112*, 813-823.

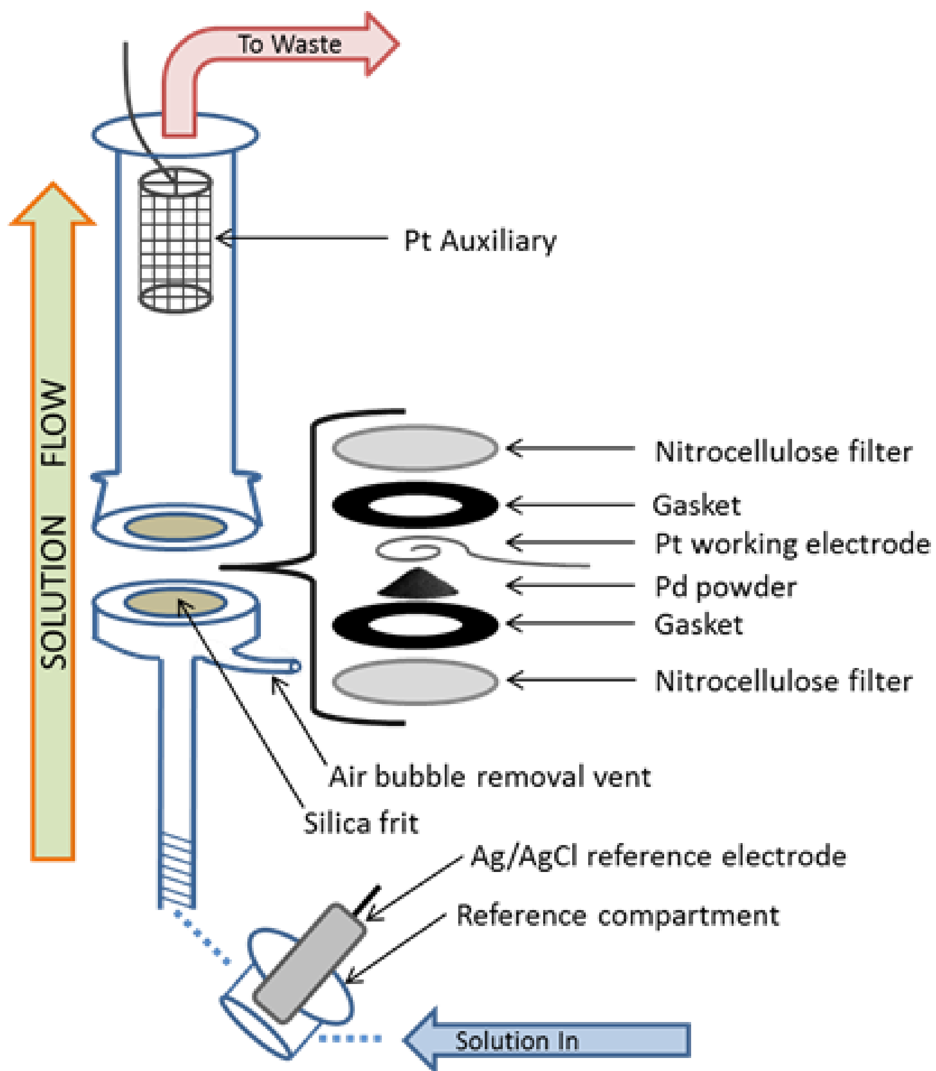

Figure 2.1: Powder flow cell

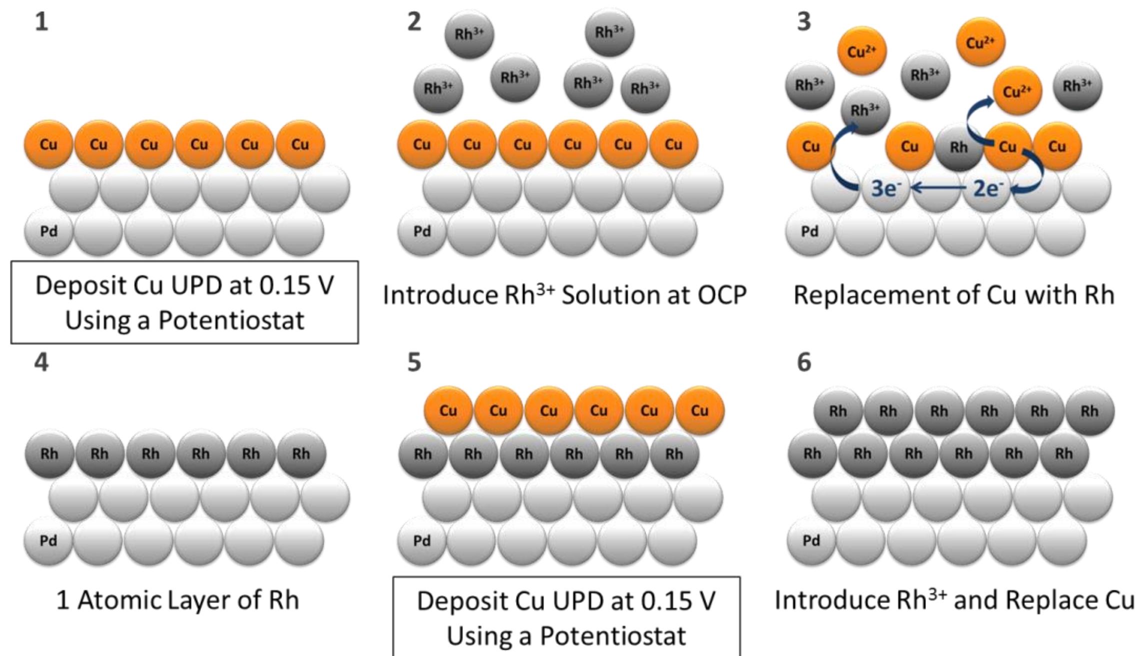

Figure 2.2: Rh deposition by SLRR

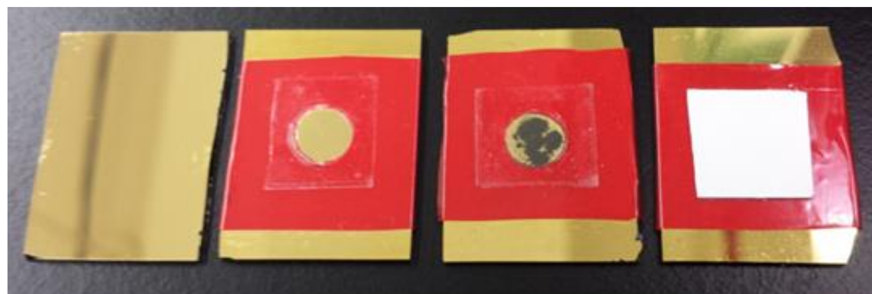

1. Gold slide
2. Add tape with punched hole
3. Add 1 mg Pd powder
4. Add nitrocellulose membrane

Figure 2.3: mg-scale powder experimentation method.

Table 2.1: Pd powder estimated surface area

Assumed values	Mass of powder sample		50 mg
	Particle diameter (um)		1 um
	Particle radius (cm)		0.00005 cm
Known value	Pd density (g/cm^3)		12 g/cm^3
Calculations	Volume of a particle, $(4/3)\pi r^3$		5.2E-13 cm^3/particle
	Surface area of a sphere, $4\pi r^2$		3.1E-08 cm^2/particle
	Volume of powder sample	(m_{Pd}/d_{Pd})	4.17E-03 cm^3 powder
	Number of particles	$V_{sample}/V_{particle}$	7.96E+09 particles
	Surface area of sample	$\#_{particles} * A_{particle}$	250 cm^2
			=0.50 m^2/g

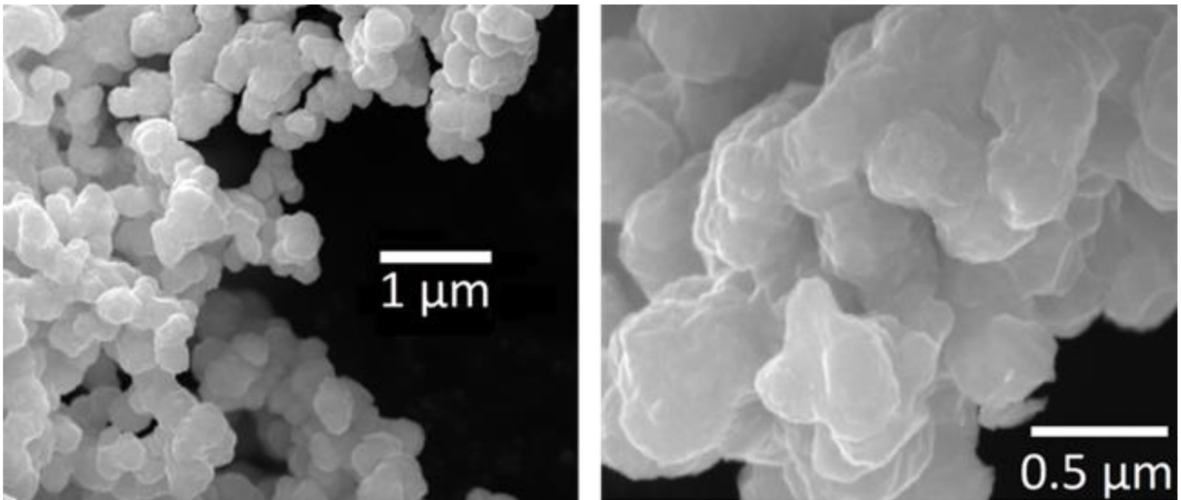

Figure 2.4: SEM images of unmodified Pd powder particles at two different scales.

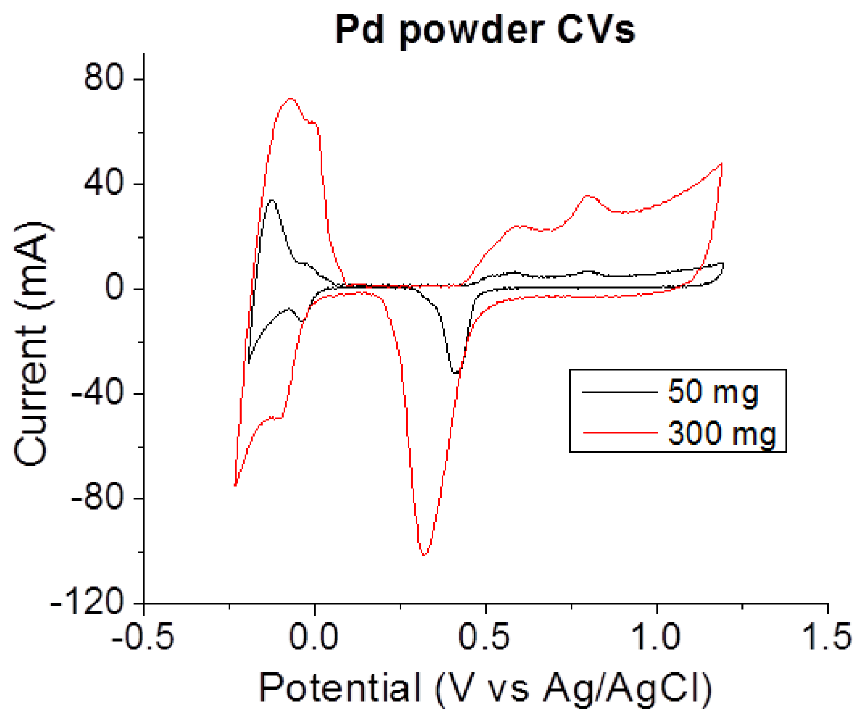

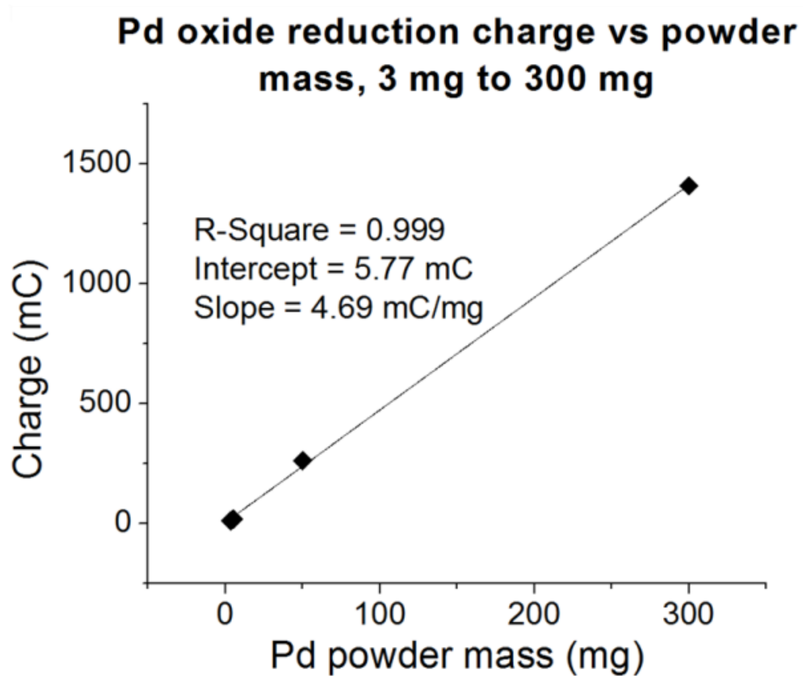

Figure 2.5: Pd powder CVs (top), and oxide reduction peak charges (bottom). 10 mV/s scan rate.

Table 2.2: Comparison of Pd oxide reduction peak charge and calculated surface area for various samples. Surface area is normalized against the 2 cm^2 Pd on Si wafer, by assuming that it represents complete Pd surface coverage.

Pd oxide reduction peak charge for surface area comparison vs Pd on Si		
Sample	*Charge (mC)*	*Normalized surface area (cm^2)*
Pd on Si wafer (2 cm^2)	2.5	2
15 cycle Pd SLRR on Au film (2 cm^2)	2.2	1.8
3.5 mg Pd powder	12	9.6
5 mg Pd powder	19.5	16
50 mg Pd powder	262	210
300 mg Pd powder	1410	1130

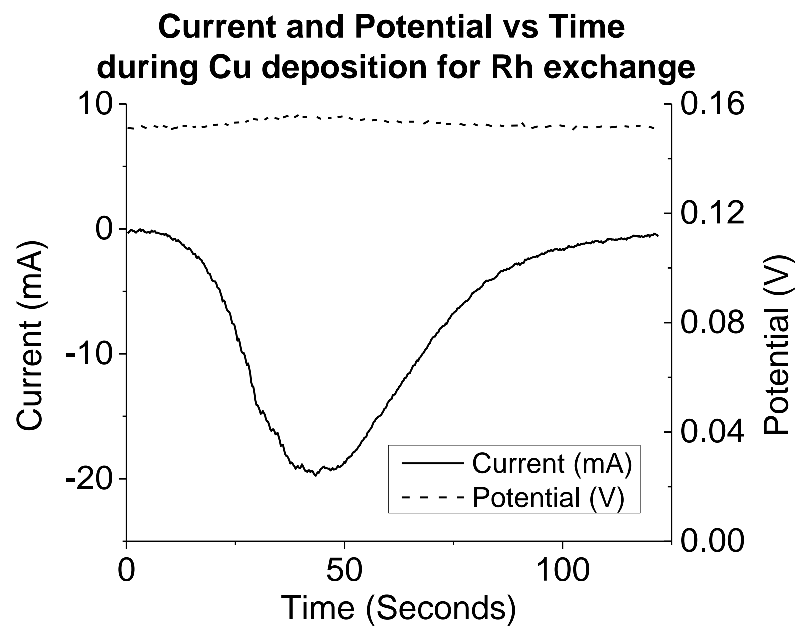

Figure 2.6: Current (solid line) and potential (dashed line) during Cu deposition on Pd powder.

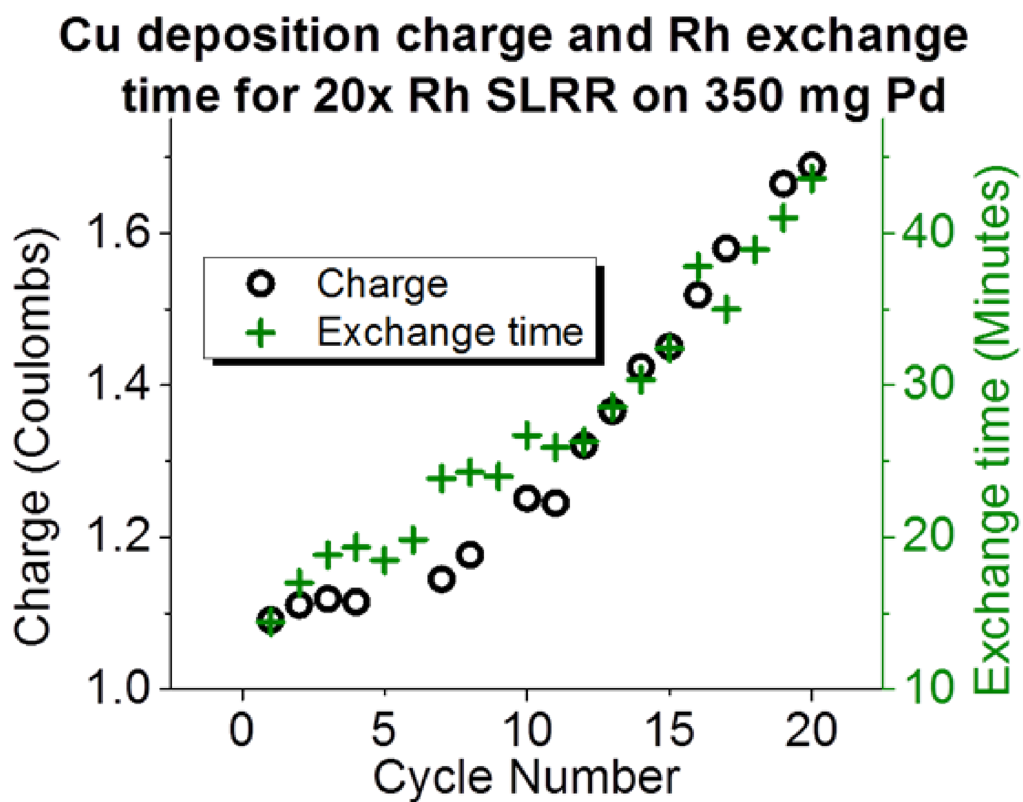

Figure 2.7: Plot of Cu deposition charge (black circles) and exchange time (green crosses) for a 20 cycle Rh deposition by SLRR on 350 mg Pd powder.

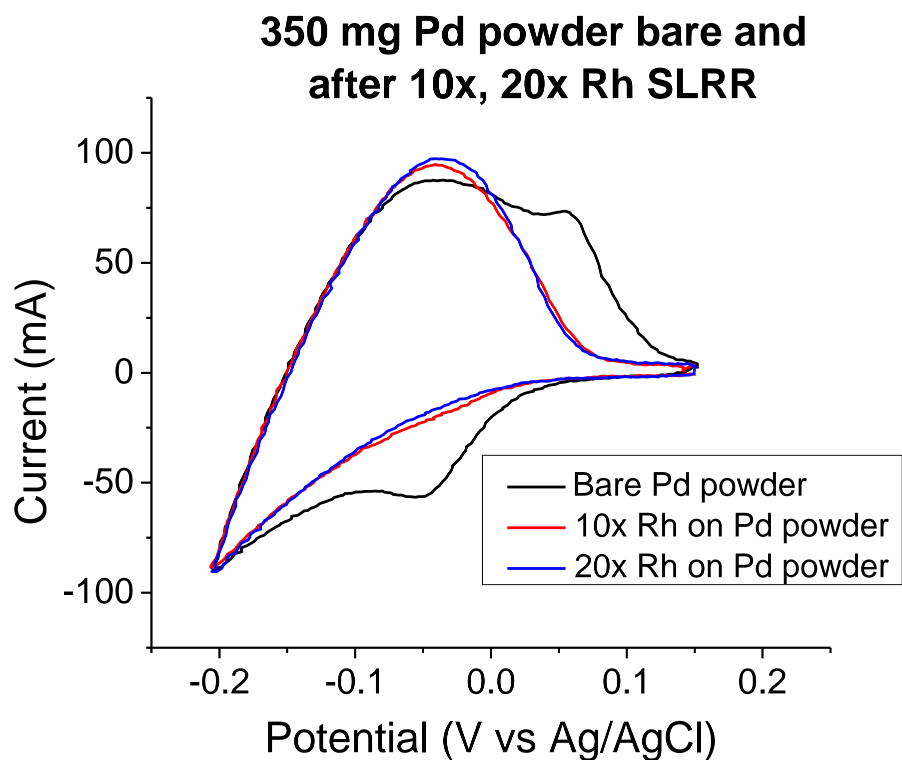

Figure 2.8: Overlaid CVs of 350 mg bare Pd (black), then modified by 10 (red) and 20 (blue) cycles of Rh SLRR.

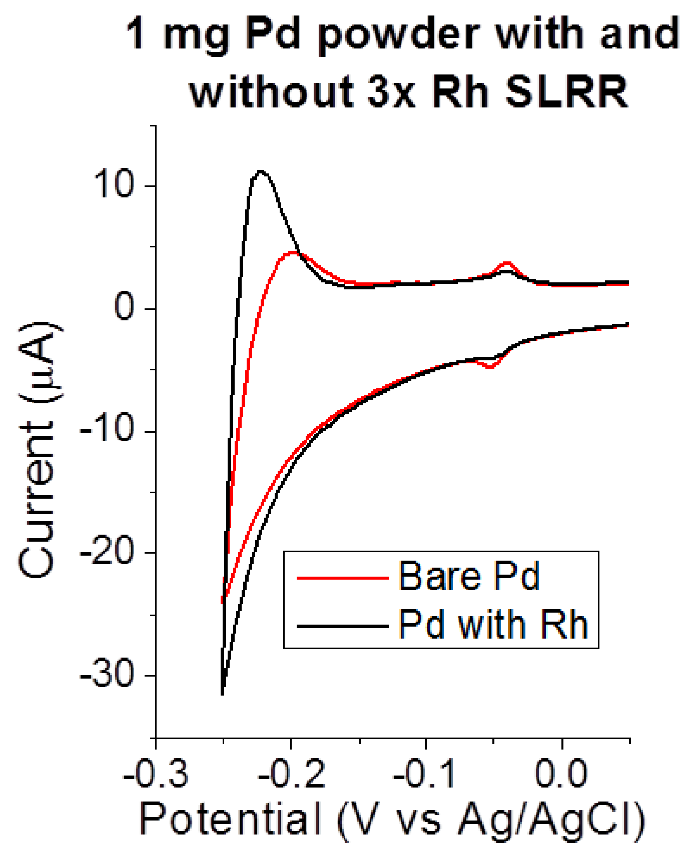

Figure 2.9: CV of Pd powder bare (red) and modified by 3 cycles of Rh SLRR (black).

10 mV/sec scan rate.

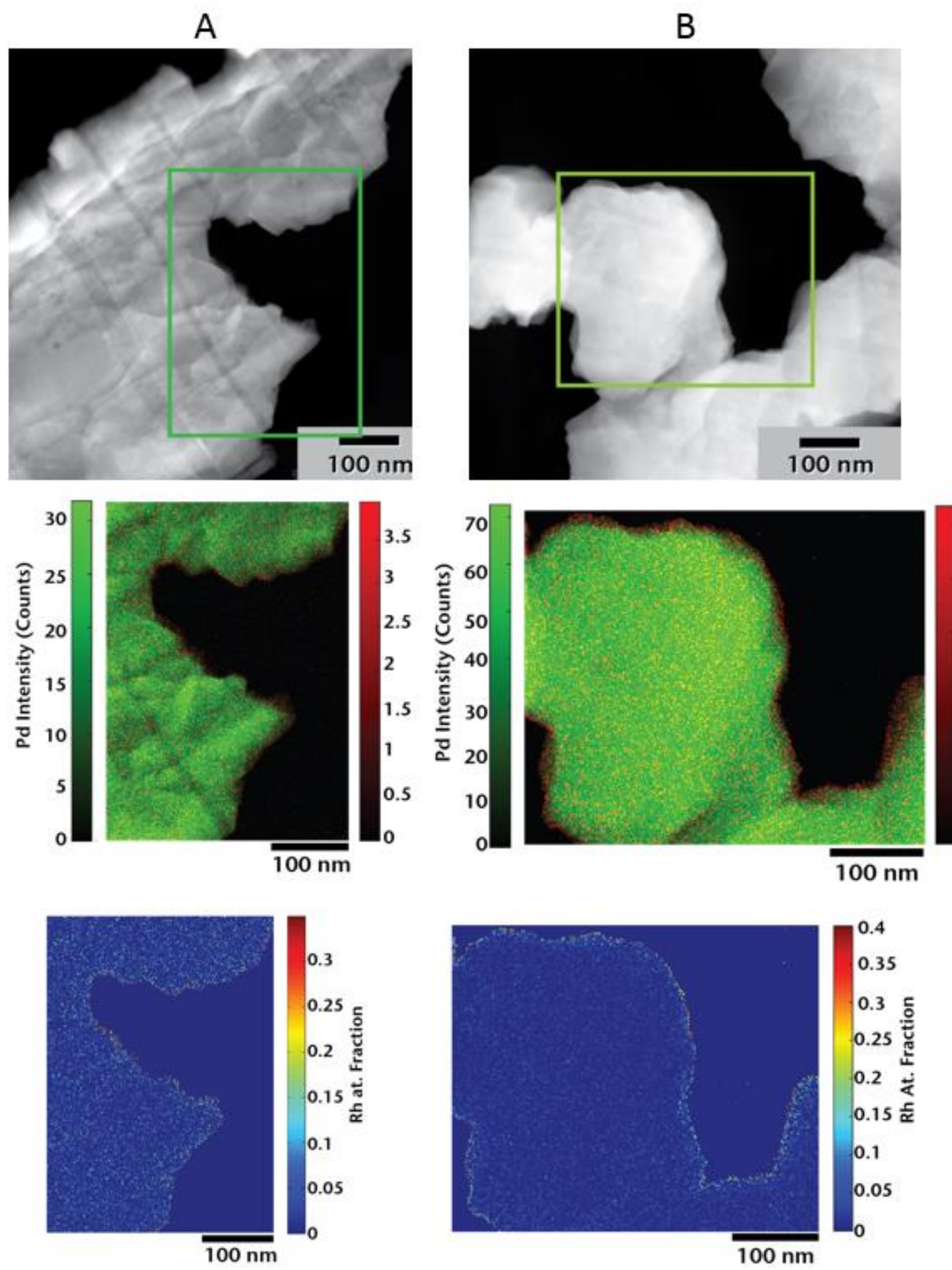

Figure 2.10: (Top) high-angle annular dark field scanning transmission electron micrograph, (middle) STEM-EDS rhodium (red) and palladium (green) overlay map, and (bottom) Rh atomic fraction map of (A) 1x Rh on Pd, and (B) 6x Rh on Pd. Scale bars are 100 nm.

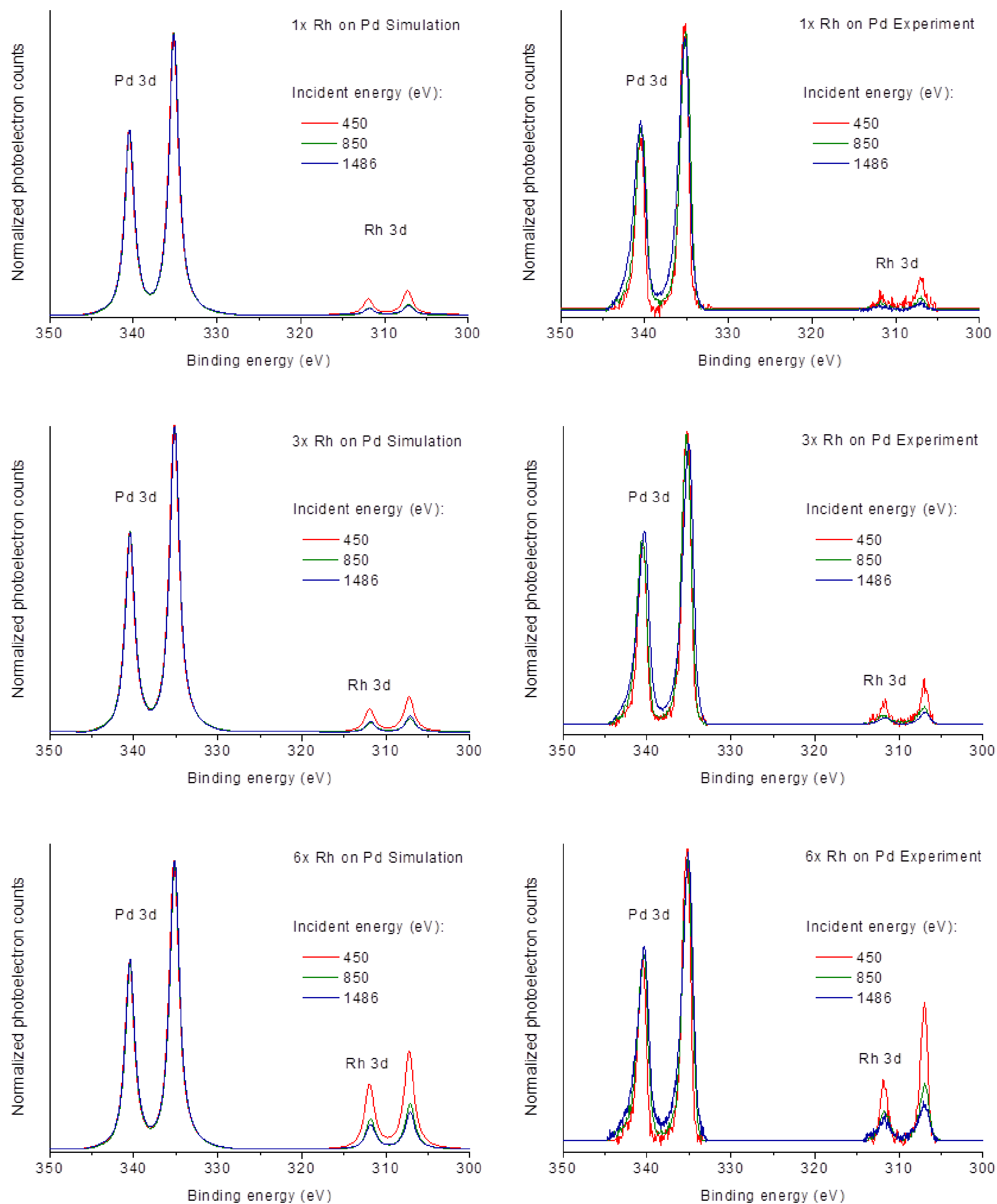

Figure 2.11: Experimental and simulated spectra at 450, 850, and 1486 eV for, top to bottom, 1, 3, and 6 cycles of Rh deposited on Pd powder. All spectra were background-subtracted and normalized to the area of the Pd peaks.

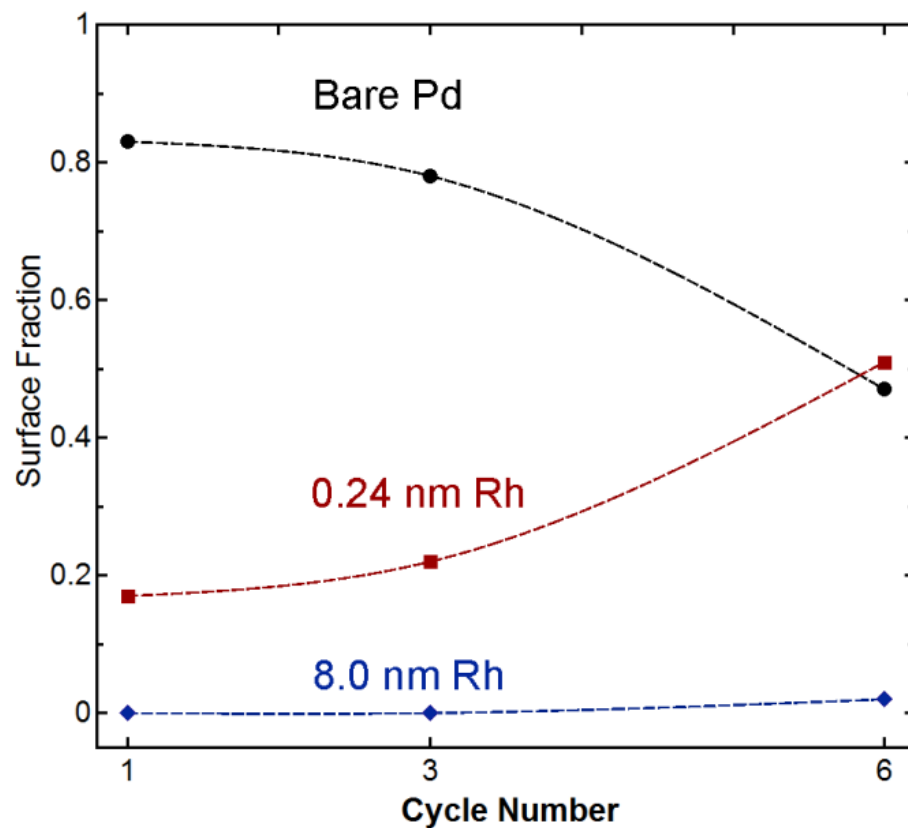

Figure 2.12: Contributions of each component to the best-fit simulation for each sample.

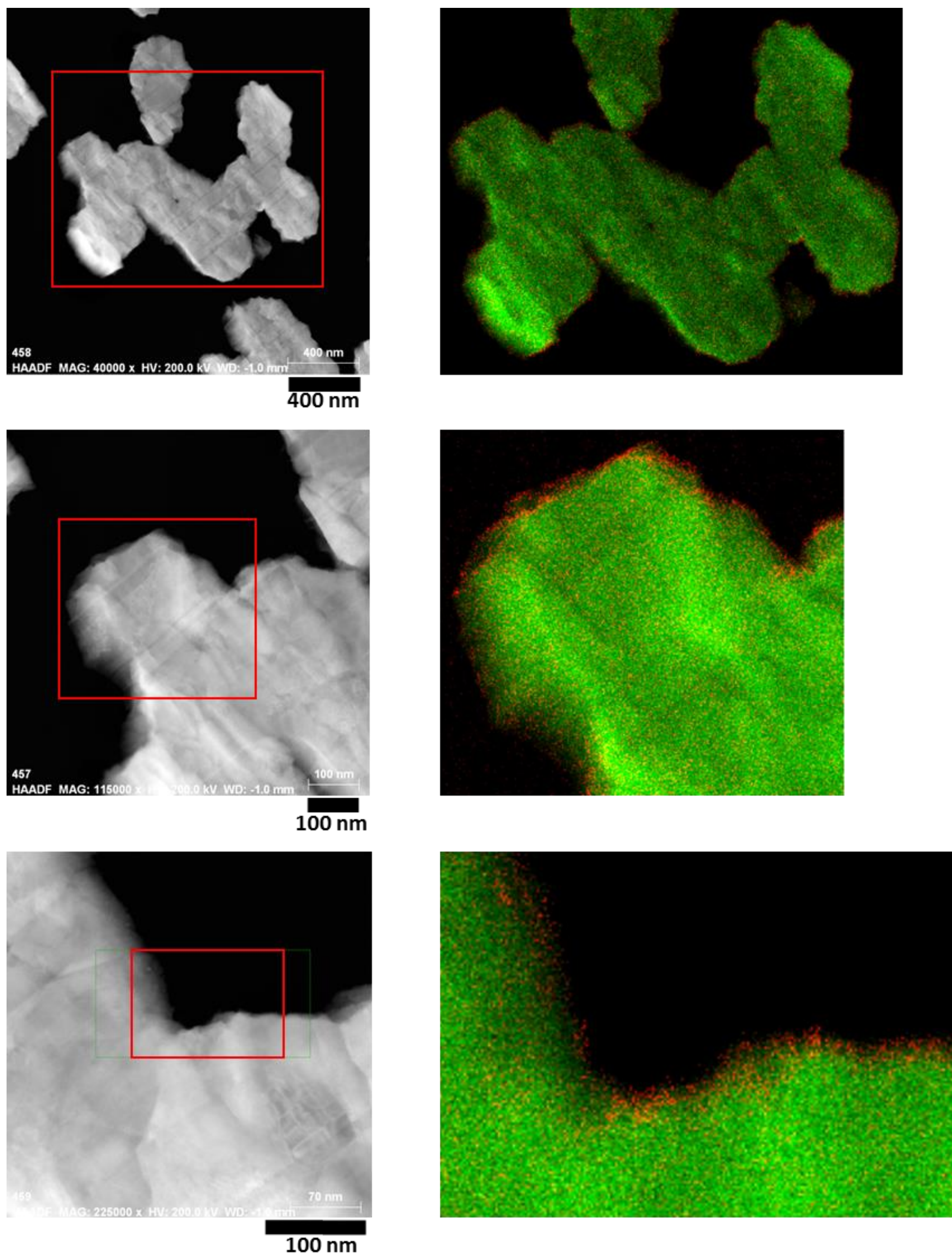

Figure 2.13: High-angle annular dark field scanning transmission electron micrograph (left column) and STEM-EDS platinum (red) and palladium (green) overlay map (right column) of 6x Pt on Pd.

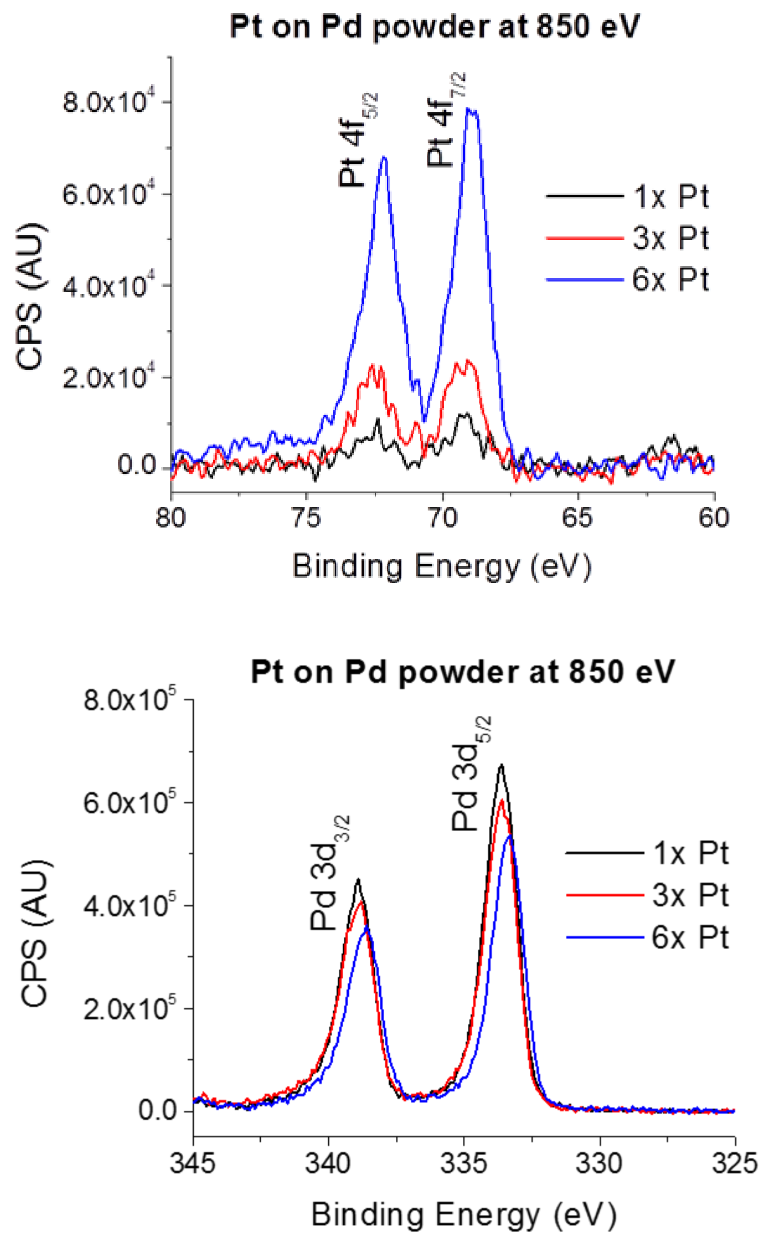

Figure 2.14: XPS data shows increasing Pt signal (top) and decreasing Pd signal (bottom) with increasing deposition cycles.

Table 2.3: XPS peak area comparison for Rh and Pt by number of deposition cycles.

Normalized XPS peak areas for deposited metals					
	Rh: 3d peak area			Pt: 4f peak area	
Excitation energy	450 eV	650 eV	850 eV	450 eV	850 eV
1x SLRR	185	162	89	143	29
3x SLRR	288	287	123	318	81
6x SLRR	955	1073	414	1217	296

CHAPTER 3

ATOMIC-LAYER ELECTROLESS DEPOSITION IN A FLOW CELL[1]

---

[1] D. Benson, K. Jagannathan, D. Robinson, and J. Stickney, To be submitted to *Journal of the Electrochemical Society (2015)*

Abstract

The goal of this study is to evaluate whether the flow cell platform can be used to implement a version of the atomic layer electroless deposition (ALED) procedure reported in our 2014 *Langmuir* paper. ALED is an electroless analog to electrochemical atomic layer deposition (E-ALD). Where E-ALD uses surface limited redox replacement (SLRR) of underpotential deposition (UPD) amounts of a sacrificial metal such as Cu, ALED uses dissolved hydrogen to form a surface hydride which is exchanged to deposit the metal ion of interest an atomic layer at a time. Deposits created are studied by cyclic voltammetry (CV) and linear sweep voltammetry. CV results show results consistent with successful deposition of Pd and Rh in a layer by layer manner. Linear sweep voltammetry is used to strip the deposit from the substrate in order to integrate the charge associated with the ions leaving the surface. It is determined that ALED deposits Pd at about 1/8 the rate of E-ALD. In summation, ALED is shown to be effective in a flow cell for the deposition of Pd on a Pd seed layer, as well as for deposition of Rh on Pd.

Introduction

Palladium is a continued source of scientific interest in areas that include hydrogen storage, fuel cells, sensors, and catalysts.[1-4] Deposition of atomic-scale layers of other metals has been targeted as a promising method to achieve improved properties for these materials.[5-8] Atomic layer deposition is a gas-phase technique that is commonly used to achieve atomic-scale growth by using surface limited reactions in a cycle,[9] but it suffers the drawbacks of requiring high temperature and high vacuum. Electrochemical atomic layer deposition (E-ALD) is a condensed phase equivalent of ALD that is carried out using ambient operating conditions that has been used to deposit numerous elements

on several substrates.[10] E-ALD has the advantage of its unrestrictive operating conditions, but requires that the substrate be in electrical contact to an instrument to control the potential. The amount of current required from the instrument scales with the surface area of the substrate. This limits the applicability of E-ALD as it pertains to materials with high surface areas or materials on non-conducting substrates.

A new technique, atomic layer electrodeposition (ALED), has been introduced that yields atomic-scale material growth at ambient conditions and that does not require electrical connection.[11] As it was initially reported, ALED used H_2 gas at a specific partial pressure being bubbled into a vessel containing the substrate immersed in solution to form a surface hydride, and then adding aliquots of metal ion precursor and exchanging the hydride by reducing the metal. The cycle was repeated to grow the deposit in thickness. This process is similar to E-ALD. E-ALD utilizes an electrochemical surface limited reaction called underpotential deposition (UPD).[12-16] UPD creates a deposit of an atomic layer, with no more than one monolayer (ML), defined here as one adsorbate atom per substrate atom. The UPD metal is exchanged at open circuit for a more noble metal,[17-19] in a surface limited redox replacement (SLRR), creating a deposit limited by the amount of sacrificial metal present. The E-ALD cycle is completed after a rinse with blank solution. Repeating the cycle increases deposit thickness.[20-22] SLRR using UPD hydrogen has been reported recently as the first example of a nonmetal used as a sacrificial element.[23] An electroless deposition method for atomic layer deposition has been introduced in a technique called electroless surface limited redox replacement (ESLRR).[24,25] ESLRR, however, uses electroless formation of a UPD layer of a metal to then exchange for the more noble metal ion of interest. ALED

combines desirable features from both of these: a nonmetal element for exchange, and a completely electroless deposition process.

In order to be able to automate the growth procedure, the ALED process was herein modified to operate in a flow cell. In this modified technique, ALED began by creating an adsorbed layer of hydrogen from a sparged solution of H_2 gas dissolved in blank. The solution was then exchanged, at open circuit, for one containing ionic precursor for the element to be deposited, Rh or Pd. The ion of interest was reduced by electrons from the adsorbed hydrogen, which acted as a sacrificial layer and was rinsed away as protons. The coverage of the sacrificial adsorbed hydrogen layer limited the amount of elemental deposition. The ionic precursor solution was rinsed out with a blank solution to complete the cycle. The cycle was repeated a number of times to grow deposits of desired thickness. In addition to providing automation, using a flow cell to create ALED deposits will also allow a direct comparison to E-ALD flow cell deposits. The deposits were analyzed by cyclic voltammetry (CV) and by linear voltammetry stripping for charge integration.

Experimental Methods

All solutions were prepared using 18 MΩ-cm water from a water filtration system (Milli-Q Advantage A10). Hydrogen gas was 1% in Ar (Airgas). The Pd solution was 0.1 mM ultrapure-grade $PdCl_2$ (Aldrich) in 50 mM HCl (Fischer Scientific) and 0.1 M H_2SO_4 (Fisher Scientific, analytical grade). The Rh solution contained 0.1 mM $RhCl_3$ (Sigma-Aldrich, 99.9%, trace metals basis) in 0.1 M H_2SO_4. The sacrificial metal solution for E-ALD was 2 mM $CuSO_4$ (J.T. Baker, 99.8%) in 0.1 M H_2SO_4. For ALED, the sacrificial hydrogen solution was 0.1 M H_2SO_4 which was sparged with the 1% H_2 in

Ar for at least 2 hours. The blank solution was 0.1 M H_2SO_4. Prior to use, all solutions, except for the H_2 solution, were degassed with N_2 for one hour to remove dissolved O_2.

Experiments were performed using an automated flow cell system (Electrochemical ALD, L.C.) consisting of a variable speed pump, a solenoid selection valve, solution reservoirs, a potentiostat, and a three electrode flow cell (Figure 3.1). Sequencer 4.0 control software (Electrochemical ALD, L.C.) was used for making the deposits. Solutions were sucked from bottles, through the valve block, and upward through the cell before being pumped into the waste. The gold electrode used was polycrystalline Au on glass purchased from Evaporated Metal Films. The substrate surface area for deposition was 2 cm^2. All potentials are reported vs the Ag/AgCl (3 M KCl) reference electrode (Bioanalytical Systems, Inc.). All cyclic voltammograms were collected at a scan rate of 10 mV/sec in 0.1 M H_2SO_4. Solution flow rate during deposition cycles was 17 mL/min. During CVs, the flow rate was 2 mL/minute.

As illustrated in Figure 3.2, the ALED procedure began as hydrogen (1% in Ar) gas was bubbled through 0.1 M H_2SO_4 to create a hydrogen saturated solution. This solution was flowed over a Pd film on gold to cause hydrogen sorption. The Pd film was prepared by 5 cycles of electrochemical atomic-layer deposition. The hydrogen solution was flowed over the substrate for 60 seconds, where the desired potential was reached. The substrate was then exposed to Rh solution at open circuit for 45 seconds, allowing the Rh to exchange for the adsorbed hydrogen, resulting in Rh deposition on the Pd surface. After the Rh exchange step, the cell was rinsed for 60 seconds with blank, completing the cycle. This cycle was repeated the desired number of times to create various deposit thicknesses (see schematic cartoon, Figure 3.2). The method for growing

films using surface limited redox replacement (SLRR) has been reported previously.[8] It is similar to the ALED method but uses an electrochemically deposited UPD layer of Cu as the sacrificial element.

The ALED procedure was also used to deposit Pd in the same manner as Rh. Rather than depositing on a 5 cycle Pd SLRR substrate, however, the Pd deposits were grown on a 1 cycle Pd SLRR substrate to mimic growth on a seed layer. The Pd deposits were examined by cyclic voltammetry in order to observe the response to increasing the number of deposition cycles. Additionally, the deposited Pd was stripped electrochemically using linear sweep voltammetry. In order to strip the Pd, the potential was ramped from 150 mV to 750 mV at a rate of 5 mV/s in HCl solution and the resulting charge was integrated in order to determine the amount of Pd that was being deposited with each cycle. The Pd stripping charge was integrated using the "Integrate" tool in OriginPro 9.0.

Results

In order to optimize the deposition cycle, the potential at the Pd substrate was observed as a function of flow time using the dissolved H_2 solution (Figure 3.3). It was observed that the potential reached a plateau at -0.225 V after about 50 seconds of solution flow, after which point the potential would not drop further. For this reason, a flow time of 60 seconds was used during each cycle to ensure H saturated the Pd consistently prior to exchange for the metal salt.

A potential-time trace for a Pd deposition cycle using ALED is shown in Figure 3.4. In this figure, a hydride formation potential of 0 V had been used. After the initial rise in potential due to clearing blank solution through the tubes during approximately the

first 4 seconds, the potential is shown decreasing as the solution containing dissolved H_2 reaches the cell until a time of about 15 seconds. Upon reaching 0 V, blank flowed for 1 second to rinse the H_2 solution from the cell, before solution flow was switched to the Pd^{2+} solution for 10 seconds, then stopped. The increase in potential occurs as Pd^{2+} ions are reduced onto the substrate. The solution was held in the cell for 45 seconds to ensure the exchange was complete, as evidenced by the plateau in the potential around 425 mV. The Pd-containing solution was then rinsed from the cell with blank for 60 seconds, before the cycle was repeated.

Pd Deposition

A substrate of 1 cycle of Pd SLRR was scanned by cyclic voltammetry to provide a baseline for subsequent deposition of Pd by ALED (Figure 3.5). Scans were obtained by sweeping from the initial potential of +150 mV negative to -300 mV, and then reversing direction and sweeping back to +150 mV. 1, 5, 10, and 15 cycles of electrolessly deposited Pd are plotted. With the first cycle (red), the hydrogen absorption and desorption peaks near -250 mV are seen to increase in size, indicating that the Pd is growing in thickness, allowing a greater amount of H to absorb. As with CV of the single Pd SLRR substrate layer, the H waves which typically appear at 0 V are not yet apparent, indicating that the surface coverage remains low. As the number of deposition cycles increases to 5, 10, and 15, the H waves at 0 V grow in size, indicating an increasing surface coverage with Pd as more H is able to adsorb. As the adsorption peak grows as the number of cycles increases from 10 to 15, it can be understood that the surface is still not completely covered with Pd after 10 cycles. Similarly to the continued

increase in adsorption peak size, the H absorption and desorption peaks around -250 mV continue to grow as the increased Pd thickness allows greater amounts of H absorption.

Linear sweep voltammetry was used to strip the Pd from the Au surface of one sample after 12 Pd ALED cycles (Figure 3.6). The charge from the Pd leaving the surface was integrated for a total of 1355 μC, which gave an average charge of approximately 55 $\mu C/cm^2$ per deposition cycle. Using the established value of 220 $\mu C/cm^2$ for a 1 ML[26] deposit on Au for a 1 e^- process and taking into account that $Pd \rightarrow Pd^{2+} + 2 e^-$ is a 2 electron process, it is estimated that each ALED cycle deposited about 1/8 ML (0.12 ML) of Pd. It has previously been established that Pd grown using E-ALD deposits 0.8 ML per cycle.[21] Comparing these values indicates that ALED for Pd deposits about 15% of the amount of material compared to E-ALD.

Rh Deposition on Pd

Cyclic voltammetry was performed on a bare Pd substrate for comparison once the substrate was subsequently modified with Rh by ALED (Figure 3.7). The potential was scanned beginning at +150 mV moving negative to -225 mV, then reversed and scanned in the positive direction back to +150 mV. Arrows indicate the direction of peak growth as a result of additional deposition cycles. The peaks near -200 mV in Figure 3.7 show that with continued Rh deposition cycles, hydrogen absorption occured at more positive potentials and desorption also occured more reversibly, both effects due to the kinetic enhancement provided by Rh. The simultaneous decrease in the H waves around -20 mV further evidences the surface becoming covered by Rh, causing it to behave more as a Rh surface than a Pd surface, as Rh will not adsorb H in this potential range.[8]

Conclusions

It has been demonstrated that atomic layer electroless deposition (ALED), which uses hydrogen in place of a sacrificial metal for open circuit exchange of metal ions, can be applied in the flow cell system. Nanofilms of Rh and Pd have been grown using ALED in the flow cell. Cyclic voltammetry indicated that both films behaved as expected, increasing the amount of hydrogen sorption with increasing thickness for Pd, and enhancing the kinetics of H sorption and desorption as Rh was deposited. By integrating the current obtained as a result of stripping the deposited Pd, ALED of Pd was determined to deposit about 15% as much material per deposition cycle compared to E-ALD. While it appears to result in less deposition, ALED offers the advantage of not requiring electrical contact with the substrate, making it a potentially more scalable technique for larger samples and metals supported by nonconductors. The adaptation of ALED to the flow cell will allow implementation of customizable automated cycles like those used in E-ALD. Additionally, it will allow further studies comparing ALED deposits to deposits made by E-ALD.

Acknowledgements

Acknowledgment is made of the support of the National Science Foundation, Division of Materials Research #1410109, and of the Laboratory-Directed Research and Development program at Sandia National Laboratories, a multiprogram laboratory managed and operated by Sandia Corporation, a wholly owned subsidiary of Lockheed Martin Corporation, for the U.S. Department of Energy's National Nuclear Security Administration under contract DE-AC04-94AL85000.

References

(1) Li, M.; Yang, W. F. Highly porous palladium bulk: Preparation and properties as active metal material for displacement chromatographic process. *Int. J. Hydrog. Energy* **2009**, *34*, 1585-1589.

(2) Antolini, E. Palladium in fuel cell catalysis. *Energy & Environmental Science* **2009**, *2*, 915-931.

(3) Leparmentier, S.; Auguste, J. L.; Humbert, G.; Delaizir, G.; Delepine-Lesoille, S.; Bertrand, J.; Buschaert, S.; Perisse, J.; Mace, J. R. Palladium particles embedded into silica optical fibers for hydrogen gas detection. *Proceedings of SPIE* **2014**, *9128*, 9.

(4) Shao, M. Palladium-based electrocatalysts for hydrogen oxidation and oxygen reduction reactions. *Journal of Power Sources* **2011**, *196*, 2433-2444.

(5) Bartlett, P. N.; Marwan, J. The effect of surface species on the rate of H sorption into nanostructured Pd. *Physical Chemistry Chemical Physics* **2004**, *6*, 2895-2898.

(6) Chen, X.; Burda, C. The Electronic Origin of the Visible-Light Absorption Properties of C-, N- and S-Doped TiO2 Nanomaterials. *Journal of the American Chemical Society* **2008**, *130*, 5018-5019.

(7) Greeley, J.; Mavrikakis, M. Surface and Subsurface Hydrogen: Adsorption Properties on Transition Metals and Near-Surface Alloys. *The Journal of Physical Chemistry B* **2005**, *109*, 3460-3471.

(8) Sheridan, L. B.; Yates, V. M.; Benson, D. M.; Stickney, J. L.; Robinson, D. B. Hydrogen sorption properties of bare and Rh-modified Pd nanofilms grown via surface limited redox replacement reactions. *Electrochimica Acta* **2014**, *128*, 400-405.

(9) George, S. M. Atomic Layer Deposition: An Overview. *Chemical Reviews* **2009**, *110*, 111-131.

(10) Stickney, J. L. Electrochemical atomic layer epitaxy (EC-ALE): Nanoscale control in the electrodeposition of compound semiconductors. *Advances in Electrochemical Science and Engineering* **2002**, *7*, 1-106.

(11) Cappillino, P. J.; Sugar, J. D.; El Gabaly, F.; Cai, T. Y.; Liu, Z.; Stickney, J. L.; Robinson, D. B. Atomic-Layer Electroless Deposition: A Scalable Approach to Surface-Modified Metal Powders. *Langmuir* **2014**.

(12) Adzic, R. R.: Electrocatalytic Properties of the Surfaces Modified by Foreign Metal Adatoms. In *Advances in Electrochemistry and Electrochemical Engineering*; Gerischer, H., Ed.; Wiley-Interscience: New York, 1984; Vol. 13; pp 159-260.

(13) Gregory, B. W.; Norton, M. L.; Stickney, J. L. Thin-layer electrochemical studies of the underpotential deposition of cadmium and tellurium on polycrystalline Au, Pt and Cu electrodes. *Journal of Electroanalytical Chemistry* **1990**, *293*, 85-101.

(14) Gregory, B. W.; Stickney, J. L. Electrochemical atomic layer epitaxy (ECALE). *Journal of Electroanalytical Chemistry* **1991**, *300*, 543-561.

(15) Kolb, D. M.: Advances in Electrochemistry and Electrochemical Engineering. Tobias, H. G. a. C. W., Ed.; John Wiley: New York, 1978; Vol. 11.

(16) Magnussen, O. M. Ordered Anion Adlayers on Metal Electrode Surfaces. *Chemical Reviews* **2002**, *102*, 679-726.

(17) Brankovic, S. R.; Wang, J. X.; Adžić, R. R. Metal monolayer deposition by replacement of metal adlayers on electrode surfaces. *Surface Science* **2001**, *474*, L173-L179.

(18) Herrero, E.; Buller, L. J.; Abruña, H. D. Underpotential Deposition at Single Crystal Surfaces of Au, Pt, Ag and Other Materials. *Chemical Reviews* **2001**, *101*, 1897-1930.

(19) Mrozek, M. F.; Xie, Y.; Weaver, M. J. Surface-enhanced Raman scattering on uniform platinum-group overlayers: preparation by redox replacement of underpotential-deposited metals on gold. *Analytical chemistry* **2001**, *73*, 5953-5960.

(20) Jayaraju, N.; Vairavapandian, D.; Kim, Y. G.; Banga, D.; Stickney, J. L. Electrochemical Atomic Layer Deposition (E-ALD) of Pt Nanofilms Using SLRR Cycles. *Journal of The Electrochemical Society* **2012**, *159*, D616-D622.

(21) Sheridan, L. B.; Gebregziabiher, D. K.; Stickney, J. L.; Robinson, D. B. Formation of Palladium Nanofilms Using Electrochemical Atomic Layer Deposition (E-ALD) with Chloride Complexation. *Langmuir* **2013**, *29*, 1592-1600.

(22) Thambidurai, C.; Kim, Y.-G.; Stickney, J. L. Electrodeposition of Ru by atomic layer deposition (ALD). *Electrochimica Acta* **2008**, *53*, 6157-6164.

(23) Nutariya, J.; Fayette, M.; Dimitrov, N.; Vasiljevic, N. Growth of Pt by surface limited redox replacement of underpotentially deposited hydrogen. *Electrochimica Acta* **2013**, *112*, 813-823.

(24) Ambrozik, S.; Dimitrov, N. The Deposition of Pt via Electroless Surface Limited Redox Replacement. *Electrochimica Acta* **2015**, *169*, 248-255.

(25) Ambrozik, S.; Rawlings, B.; Vasiljevic, N.; Dimitrov, N. Metal deposition via electroless surface limited redox replacement. *Electrochemistry Communications* **2014**, *44*, 19-22.

(26) Conway, B. E.; Angerstein-Kozlowska, H. The electrochemical study of multiple-state adsorption in monolayers. *Accounts of Chemical Research* **1981**, *14*, 49-56.

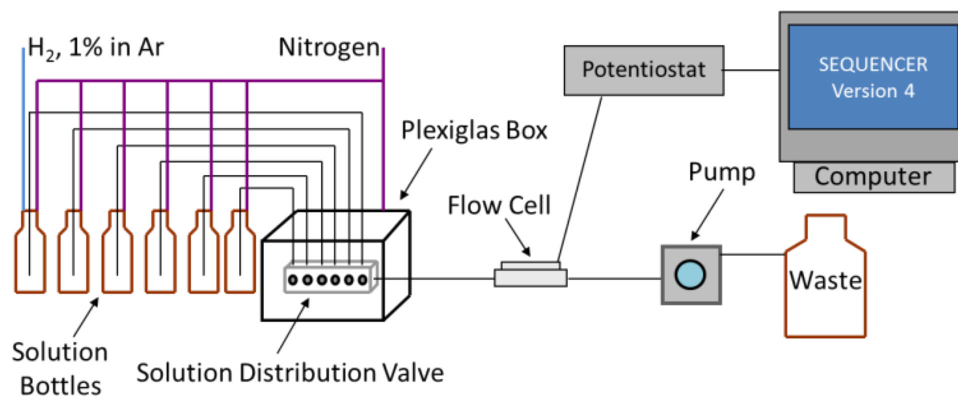

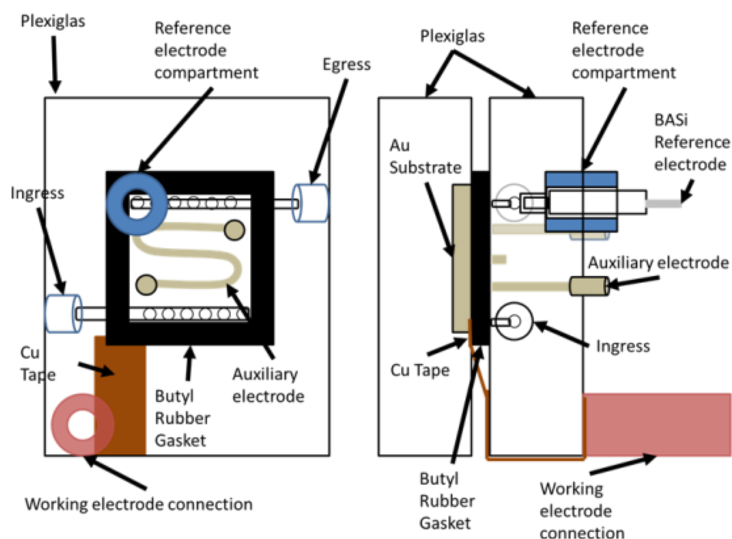

Figure 3.3: Schematic of flow cell system used for E-ALD and ALED (top) and the flow cell itself (bottom).

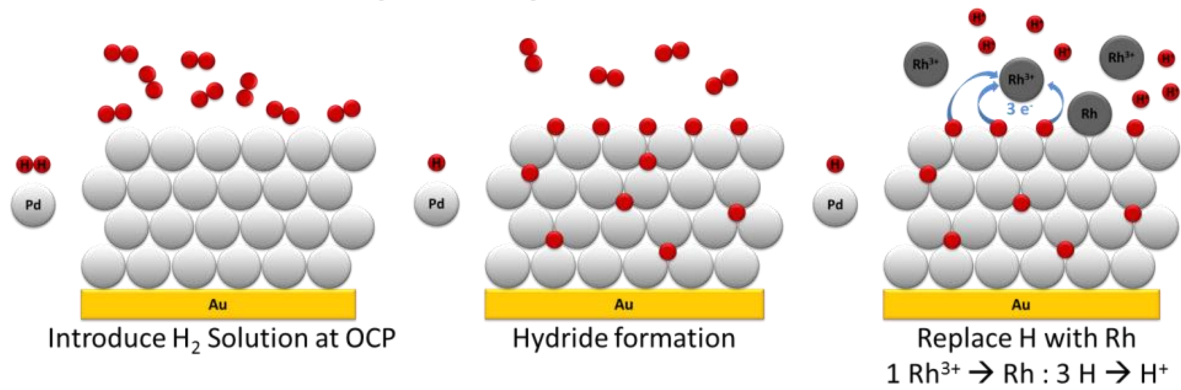

Figure 3.4: Atomic-Layer Electroless Deposition reaction scheme.

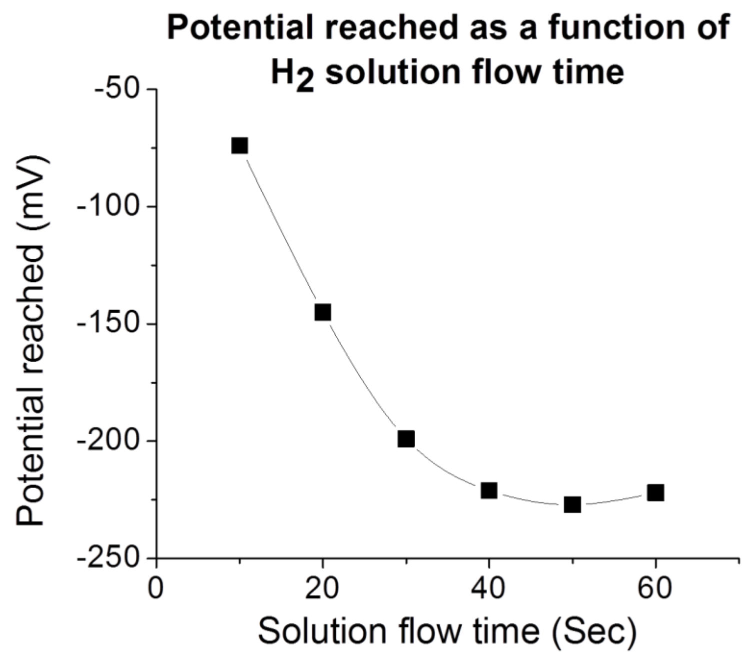

Figure 3.3: Plot of potential reached after set intervals of hydrogen solution flow.

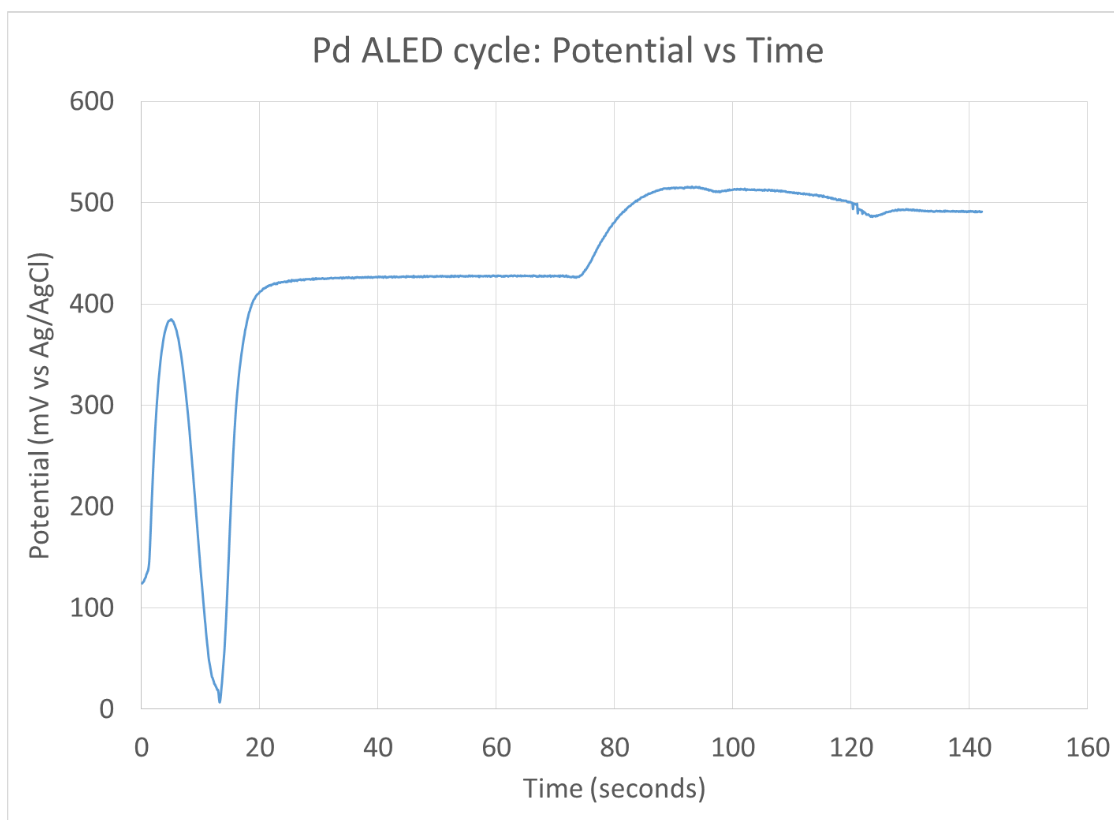

Figure 3.4: Potential-time trace for one cycle of electroless Pd deposition where the hydride formation potential used was 0 V.

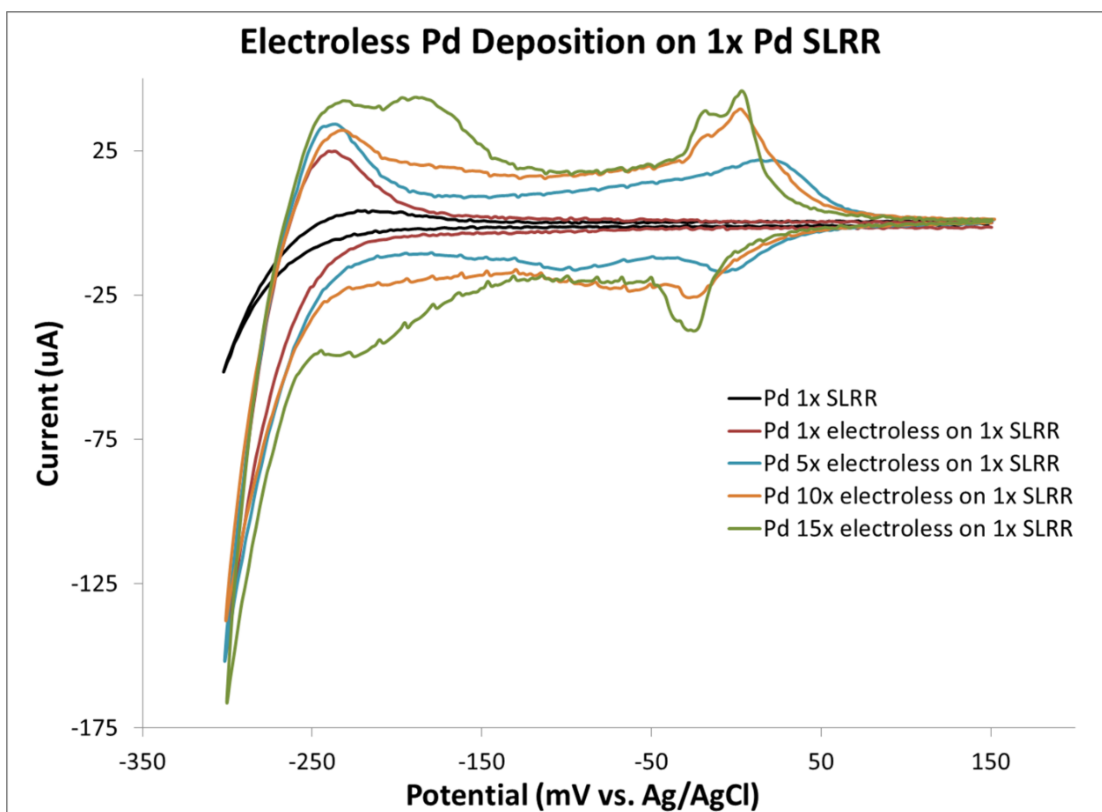

Figure 3.5: Cyclic voltammograms of increasing numbers of Pd electroless deposition cycles on a base substrate of 1x Pd SLRR on polycrystalline Au.

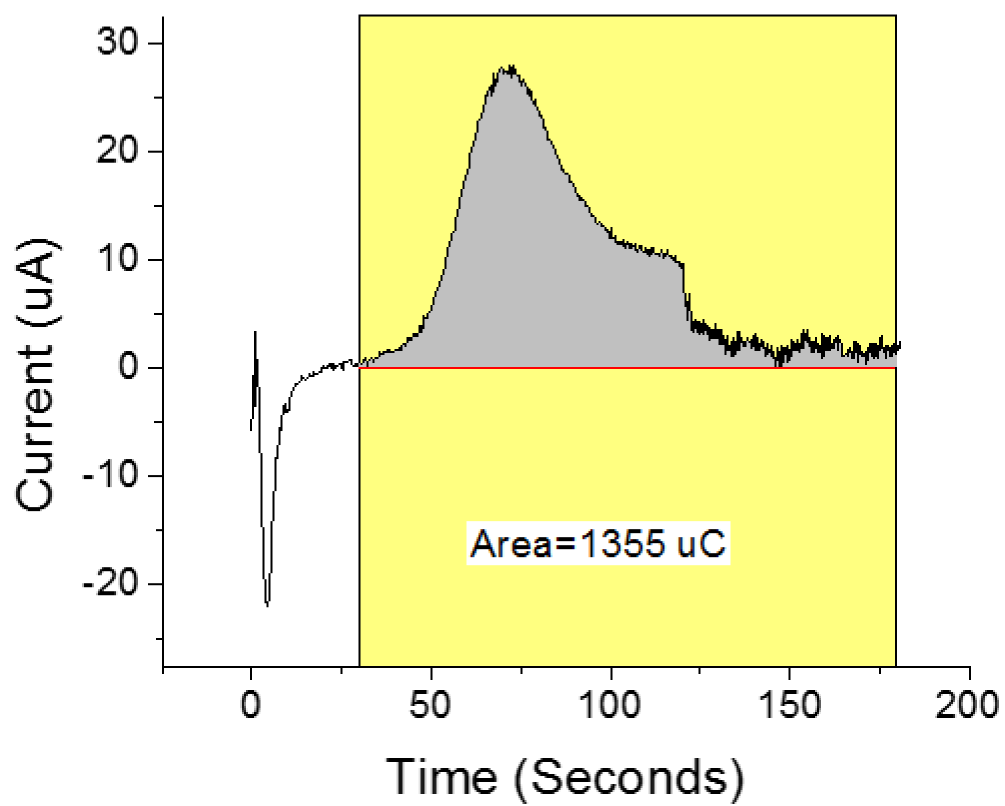

Figure 3.6: Peak integration from stripping of 12 electroless deposition cycles of Pd using H_2.

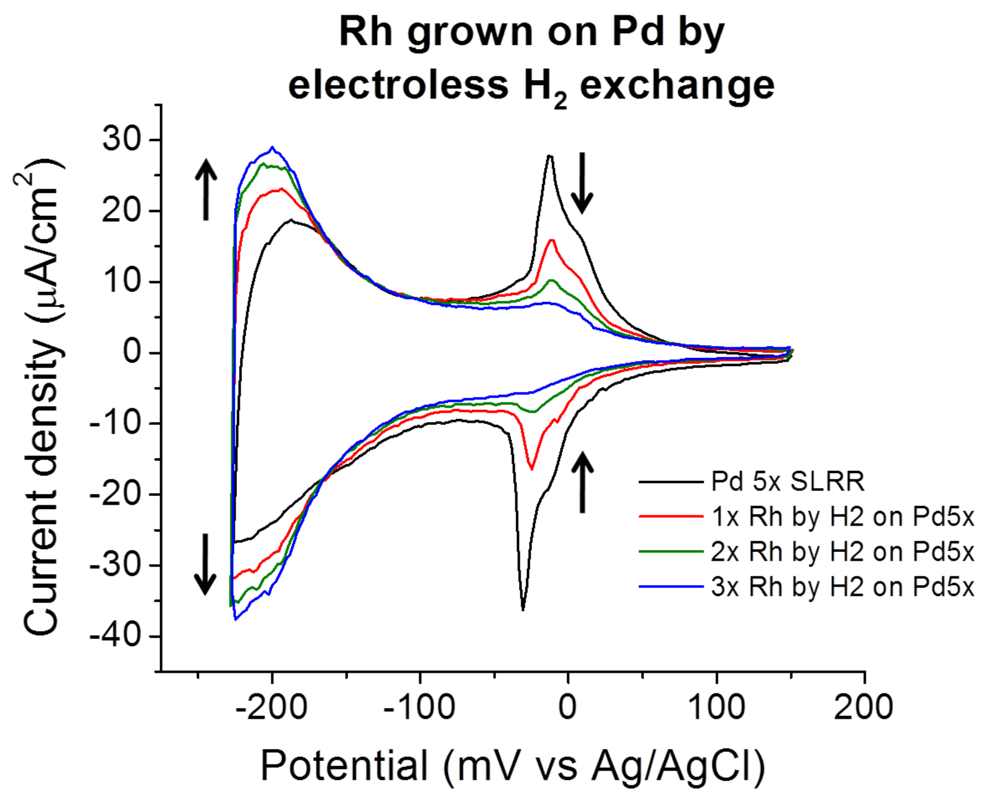

Figure 3.7: Voltammetry of Pd film with and without Rh coatings deposited by atomic-layer electroless deposition.

CHAPTER 4

HYDROGEN SORPTION KINETICS OF PALLADIUM NANOFILMS MODIFIED WITH RHODIUM DEPOSITED BY ELECTROCHEMICAL ATOMIC LAYER DEPOSITION (E-ALD) AND ATOMIC LAYER ELECTROLESS DEPOSITION (ALED)[1]

[1] D. Benson, K. Jagannathan, D. Robinson, and J. Stickney, To be submitted to *Journal of the Electrochemical Society (2015)*

Abstract

Rh-modified Pd films were generated in the flow cell system using atomic layer electroless deposition (ALED) and electrochemical atomic layer deposition (E-ALD) in order to compare the resulting deposits by each method. Voltammetric stepping was used to examine the rate of hydrogen desorption from saturated films generated by both methods. Decay curve fitting from the voltammetric profiles showed that the hydrogen desorption process occurred was best fit to a biexponential decay. This indicated that the process involved rapidly desorbing hydrogen initially, and quickly transitions to a slower rate. Surface modification with Rh increased the rate at which the hydrogen was desorbed across the Pd grown both by ALED and E-ALD, though more cycles of ALED were required to obtain the same rates as E-ALD. Cyclic voltammetry results indicated that in addition to creating thinner deposits, ALED generated less surface coverage than E-ALD per cycle.

Introduction

As technology today shifts toward smaller and smaller devices, thin films become an attractive target both academically and industrially. Thin films are desirable both for different properties they can possess versus those for bulk materials, as well as for the reduced cost associated with using less material. Palladium has well studied properties for the reversible absorption and desorption of hydrogen at ambient conditions, and for catalysis of several important reactions.[1] Pd thin films have therefore been used in fuel cell catalysis,[2,3] hydrogen sensing,[4] and H storage devices.[5] All of these fields have shown potential for enhanced qualities through formation of surface layers of other metals at the atomic scale.[6-8] Previous studies have suggested that these surface layers

alter the surface hydride properties compared to Pd, and may be useful in enhancing the kinetics of hydrogen absorption and desorption.[8] Recent work in this group has shown that the kinetics for Pd can be enhanced through surface modification by addition of atomic-layer deposits of Rh using electrochemical atomic layer deposition (E-ALD).[9]

E-ALD is an aqueous analog of atomic layer deposition (ALD). E-ALD offers low cost due to operating at ambient temperature and pressure, as well as good control over deposit thickness.[10,11] E-ALD, however, requires electrical connection to the substrate in order to control the potential and create deposits. This works well for small-scale thin films, but becomes a problem for materials on non-conducting supports. Current supply also becomes problematic for samples with large surface areas such as powders or nanostructured materials as the current required to form deposits scales with surface area. A potentially more scalable deposition process, atomic layer electroless deposition (ALED), has been reported.[12] ALED is similar to E-ALD in that it creates atomic scale deposits one layer at a time by exchanging for a sacrificial element. Where E-ALD uses electrochemically deposited metal, however, ALED uses electrolessly formed hydride to exchange for the metal ion to deposit. Previous work in this group adapted ALED to operate using a flow cell system.

In the present study, samples created by both ALED and E-ALD have been analyzed in order to draw comparisons between the two deposition methods. Pd films on deposited on Au substrates and Rh films grown on Pd substrates are studied using cyclic voltammetry (CV) and voltammetric stepping. Examining the properties of the two types of deposits will give insight into possible advantages of creating modified thin films by each method.

Experimental Methods

Hydrogen gas was 1% in Ar (Airgas). The blank solution was 0.1 M H_2SO_4. The Pd solution was 0.1 mM ultrapure-grade $PdCl_2$ (Aldrich) in 50 mM HCl (Fischer Scientific) and 0.1 M H_2SO_4 (Fisher Scientific, analytical grade). The Rh solution contained 0.1 mM $RhCl_3$ (Sigma-Aldrich, 99.9%, trace metals basis) in 0.1 M H_2SO_4. For E-ALD, the sacrificial metal solution was 2 mM $CuSO_4$ (J.T. Baker, 99.8%) in 0.1 M H_2SO_4. The sacrificial hydrogen solution for ALED was 0.1 M H_2SO_4 that was sparged with the 1% H_2 in Ar for at least 2 hours. All solutions were prepared using 18 MΩ-cm water from a water filtration system (Milli-Q Advantage A10). With the exception of the H_2 solution, all solutions were degassed with N_2 for one hour prior to use to remove dissolved O_2.

All experiments were executed using an automated flow cell system (Electrochemical ALD, L.C.) that consisted of solution reservoirs, a variable speed peristaltic pump, a solenoid selection valve, a potentiostat, and a three electrode flow cell (Figure 4.1). The flow cell system was connected to a PC and operated using Sequencer 4.0 control software (Electrochemical ALD, L.C.) to create deposits. The solutions were sucked from the reservoirs, through the selection valve, to the pump, and then pushed through the flow cell before going into the waste. The reference electrode against which all potentials are reported was Ag/AgCl (3 M KCl) from Bioanalytical Systems, Inc. A butyl rubber gasket held the polycrystalline gold electrode (Evaporated Metal Films) in place within the flow cell, and created a defined surface area of 2 cm^2 for deposition. A solution flow rate of 2 mL/min was used during CVs, and a rate of 17 mL/min was used for deposition cycles.

Schematics for deposition sequences for Rh growth by E-ALD and Pd growth by ALED are depicted in Figure 4.2. Both processes have been reported previously.[9,12] The figure shows that where E-ALD uses electrochemically formed UPD of a sacrificial metal, in this case Cu, ALED instead makes use of electrolessly formed surface hydride to exchange for the metal ion of interest. Linear sweep voltammetry was used to strip Pd deposits from the Au substrate. The stripping cycle used a potential sweep from 150 mV to 750 mV at a rate of 5 mV/s in 0.1 M HCl solution. The Pd stripping charge was integrated using the "Integrate" tool in OriginPro 9.0 in order to determine the amount of Pd that was deposited per cycle.

Results

Cyclic Voltammetry

An overlay of a comparable number of total deposition cycles for ALED and E-ALD is depicted in Figure 4.3. The blue scan is a CV of 4 cycles of Pd grown by ALED on an initial layer of 1 cycle of Pd SLRR, for a total of 5 Pd deposition cycles. The orange scan is 5 cycles of Pd SLRR. CVs were typically stopped at -250 mV. The ALED sample, however, was scanned to -300 mV. Even so, the ALED sample exhibits little hydrogen adsorption near 0 V as compared to the E-ALD sample generated by SLRR. While a Au substrate would have had a current near zero, the ALED sample does show some slight peaks associated with hydrogen adsorption from the deposited Pd. The SLRR sample's larger peaks indicate greater surface coverage by the Pd. Similarly, even though the ALED sample was scanned to a more potential 50 mV more negative, the hydrogen desorption peak upon reversing the scan, while taller, has a smaller area than that for the E-ALD deposit. Overall, the increased current throughout the CV for the 5

cycle SLRR Pd is indicative of a greater amount of hydrogen adsorption and absorption. ALED can be concluded to grow less Pd per cycle in both surface area and thickness.

Kinetics

Kinetic studies were performed by charging a bare or modified Pd film with hydrogen via the sparged 0.1 M H_2SO_4 flow at -0.250 V for 5 min to ensure the Pd was saturated with H. The Pd film was prepared through 5 cycles of electrochemical atomic-layer deposition on a gold substrate. The potential was then stepped positive to 0 V and held to allow the absorbed H to desorb. The current was monitored as a function of time. The current initially spiked due to charging in addition to the desorption of H, then decayed as the hydrogen continued to desorb. An overlay of these desorption peaks is shown in Figure 4.4. The figure compares bare Pd with Pd substrates that have had various numbers of Rh SLRR cycles performed. As the number of Rh deposition cycles increased, so did the peak current reached as well as the rate at which the current returned to baseline, indicating the role of Rh in increasing hydrogen sorption kinetics in Pd. The increase in desorption rate is consistent with previous publications for surface modification by Rh[9,12] or Pt.[6] When all of the current was integrated until a return to the baseline is reached, all of the samples gave approximately the same total current, indicating that the same amount of hydrogen was desorbed from each, allowing us to conclude that the Rh was not absorbing additional hydrogen.

Removing the portion of the plot containing the charging current allowed investigation of the current decay profile (Figure 4.5). Time constants t_1 and t_2 were determined using the Exponential Fit function ExpDecay2 in OriginPro 9.0. The t_1 is the decay constant for the first, near-vertical, portion of the plot, and t_2 is for the second,

more horizontal, portion of the curve. It is possible that the initial, rapid desorption profile of t_1 is from bulk hydrogen, while the slower process is from more stable H at the surface or points of irregularity in the crystal structure. The rate of hydrogen desorption was found to be higher for all Rh modified surfaces than for bare Pd. With equal numbers of Rh deposition cycles, SLRR-grown Rh on Pd was found to have faster desorption than samples created using the electroless hydrogen method (Figure 4.6). The SLRR-grown Pd exhibits an exponential decay in time constant immediately, whereas the H_2-grown Pd requires several deposition cycles before finally dropping to a similar baseline as the SLRR method. This indicates that the H_2 growth method deposits less Rh per cycle than SLRR does.

Conclusion

Kinetic studies were performed on planar substrates of Pd grown on Au, further modified with Rh by SLRR or by ALED. CV data shows that ALED successfully deposits Pd on Pd, but does not deposit as much Pd as E-ALD in terms of both film thickness and surface area covered. Results from voltammetric stepping indicate that increasing the number of Rh deposition cycles increases the rate of H desorption, as both time constants t_1 and t_2 decrease with increasing amounts of Rh deposition. The time constants were attained by decay curve fitting where the best fit was found to be the ExpDecay2 function within OriginPro 9.0. ALED leaves room for optimization, as it does not realize the same extent of H transport kinetic increase as SLRR does per deposition cycle.

Acknowledgements

Acknowledgment is made of the support of the National Science Foundation, Division of Materials Research #1410109, and of the Laboratory-Directed Research and Development program at Sandia National Laboratories, a multiprogram laboratory managed and operated by Sandia Corporation, a wholly owned subsidiary of Lockheed Martin Corporation, for the U.S. Department of Energy's National Nuclear Security Administration under contract DE-AC04-94AL85000.

References

(1) Adams, B. D.; Chen, A. The role of palladium in a hydrogen economy. *Materials Today* **2011**, *14*, 282-289.

(2) Kang, S.; Heo, P.; Lee, Y. H.; Ha, J.; Chang, I.; Cha, S.-W. Low intermediate temperature ceramic fuel cell with Y-doped BaZrO3 electrolyte and thin film Pd anode on porous substrate. *Electrochemistry Communications* **2011**, *13*, 374-377.

(3) Lai, B.-K.; Kerman, K.; Ramanathan, S. Methane-fueled thin film micro-solid oxide fuel cells with nanoporous palladium anodes. *Journal of Power Sources* **2011**, *196*, 6299-6304.

(4) Noh, J.-S.; Lee, J. M.; Lee, W. Low-Dimensional Palladium Nanostructures for Fast and Reliable Hydrogen Gas Detection. *Sensors* **2011**, *11*, 825-851.

(5) Niessen, R. A. H.; Vermeulen, P.; Notten, P. H. L. The electrochemistry of Pd-coated MgySc(1-y) thin film electrodes: A thermodynamic and kinetic study. *Electrochimica Acta* **2006**, *51*, 2427-2436.

(6) Bartlett, P. N.; Marwan, J. The effect of surface species on the rate of H sorption into nanostructured Pd. *Physical Chemistry Chemical Physics* **2004**, *6*, 2895-2898.

(7) Chen, X.; Burda, C. The Electronic Origin of the Visible-Light Absorption Properties of C-, N- and S-Doped TiO2 Nanomaterials. *Journal of the American Chemical Society* **2008**, *130*, 5018-5019.

(8) Greeley, J.; Mavrikakis, M. Surface and Subsurface Hydrogen: Adsorption Properties on Transition Metals and Near-Surface Alloys. *The Journal of Physical Chemistry B* **2005**, *109*, 3460-3471.

(9) Sheridan, L. B.; Yates, V. M.; Benson, D. M.; Stickney, J. L.; Robinson, D. B. Hydrogen sorption properties of bare and Rh-modified Pd nanofilms grown via surface limited redox replacement reactions. *Electrochimica Acta* **2014**, *128*, 400-405.

(10) Jayaraju, N.; Vairavapandian, D.; Kim, Y. G.; Banga, D.; Stickney, J. L. Electrochemical Atomic Layer Deposition (E-ALD) of Pt Nanofilms Using SLRR Cycles. *Journal of The Electrochemical Society* **2012**, *159*, D616-D622.

(11) Thambidurai, C.; Kim, Y.-G.; Stickney, J. L. Electrodeposition of Ru by atomic layer deposition (ALD). *Electrochimica Acta* **2008**, *53*, 6157-6164.

(12) Cappillino, P. J.; Sugar, J. D.; El Gabaly, F.; Cai, T. Y.; Liu, Z.; Stickney, J. L.; Robinson, D. B. Atomic-Layer Electroless Deposition: A Scalable Approach to Surface-Modified Metal Powders. *Langmuir* **2014**.

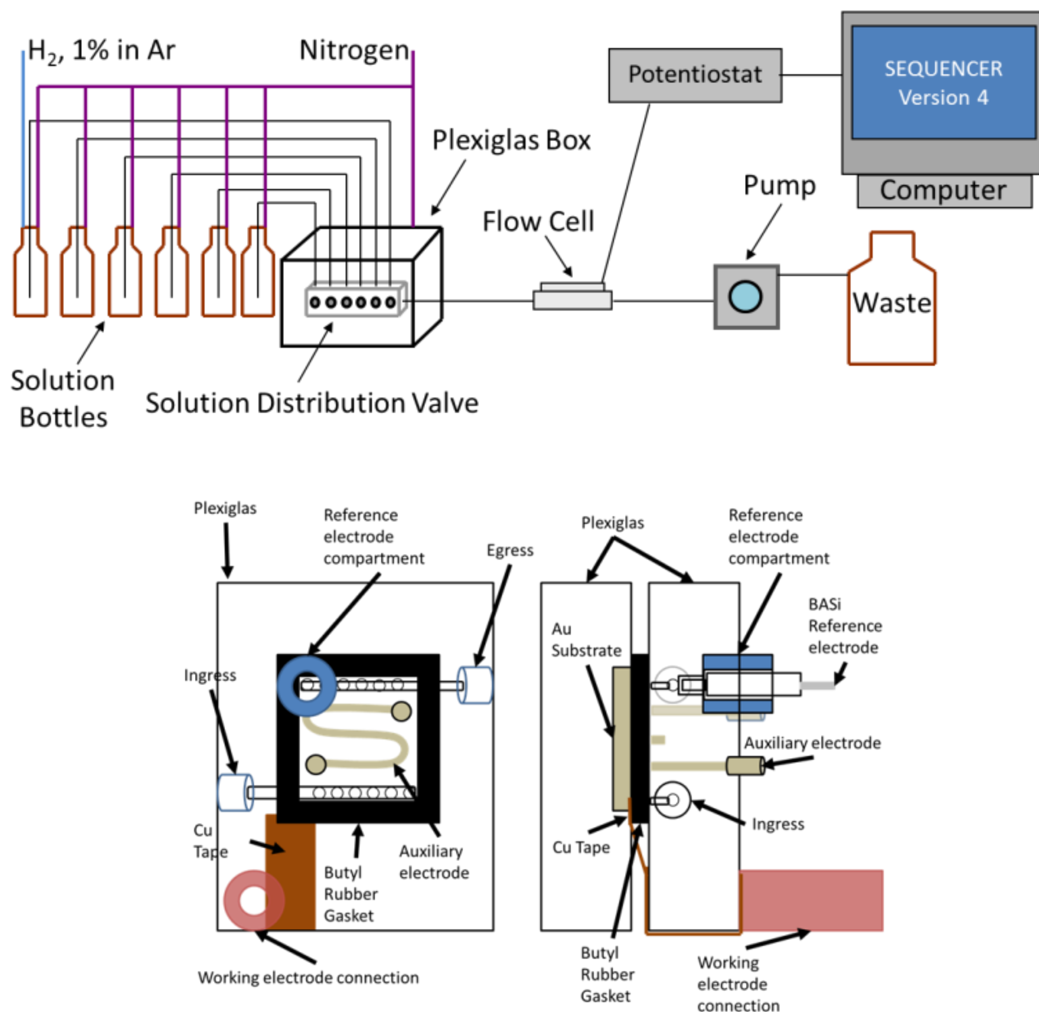

Figure 4.5: Schematic of the entire flow cell system (top) and the flow cell alone (bottom).

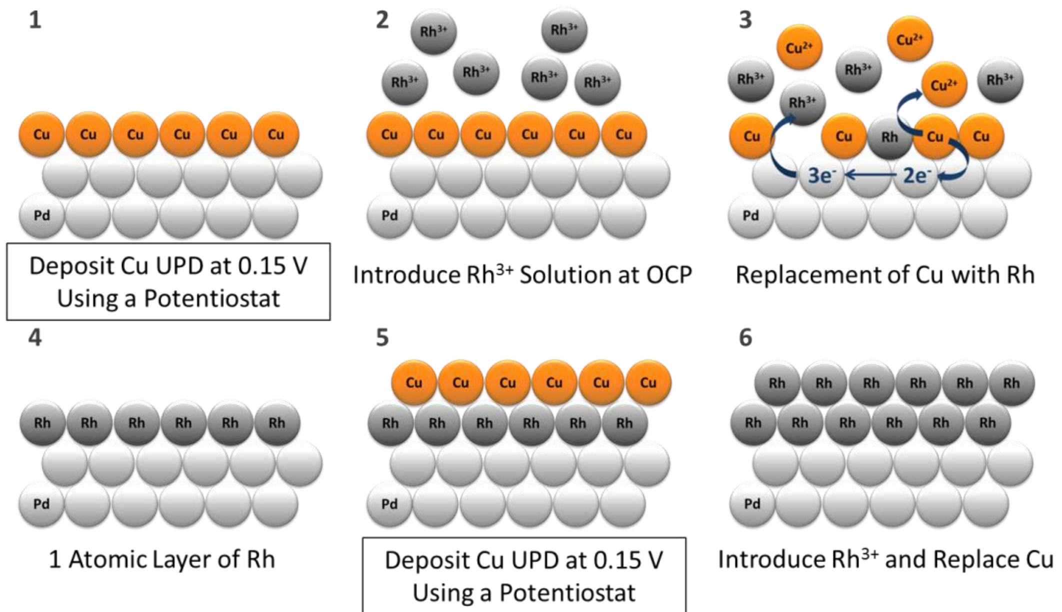

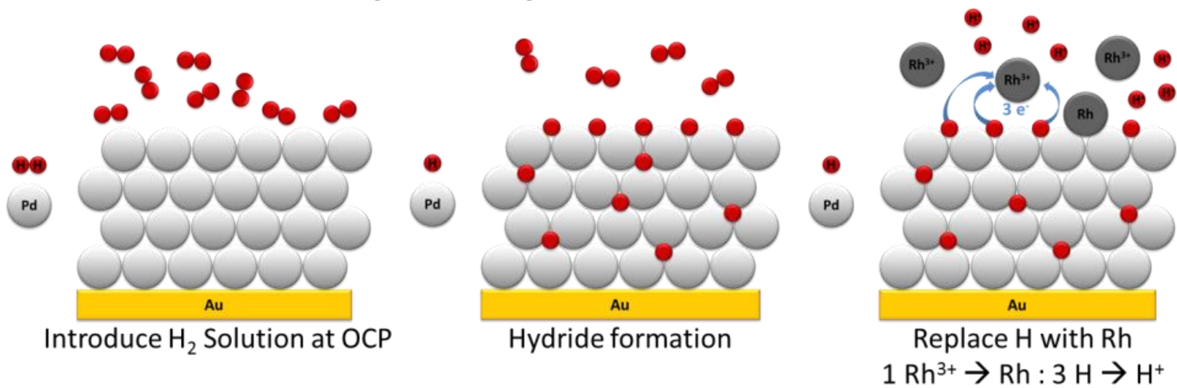

Figure 4.2: Schematics for E-ALD (top) and ALED (bottom)

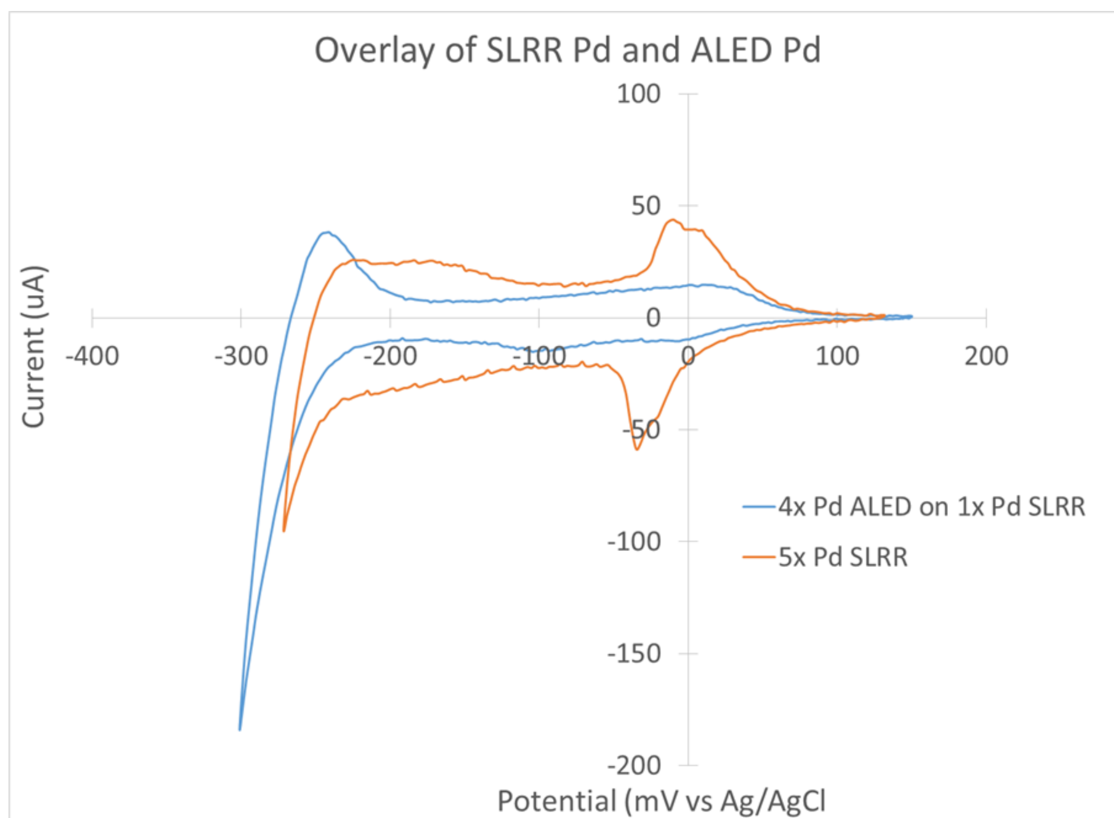

Figure 4.3: Overlay of 5 cycles of Pd grown by SLRR and 4 cycles of Pd grown by ALED on 1 cycle of Pd SLRR.

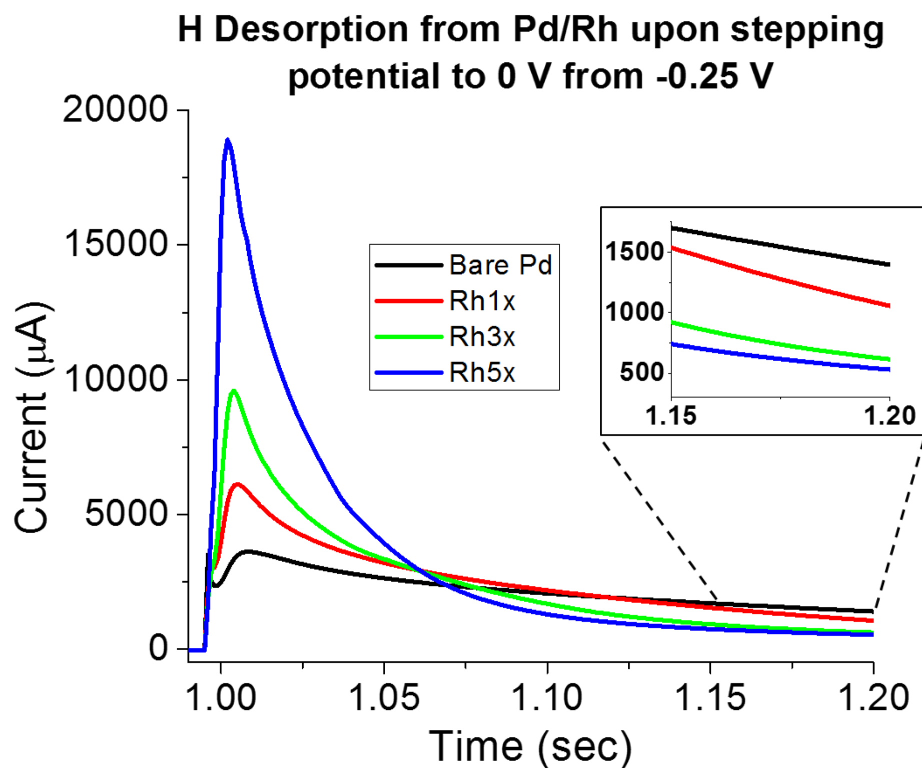

Figure 4.4: Hydrogen desorption currents induced by potential steps for films grown by electrochemical atomic-layer deposition: first 5 cycles of palladium, and then varying numbers of cycles of rhodium on palladium.

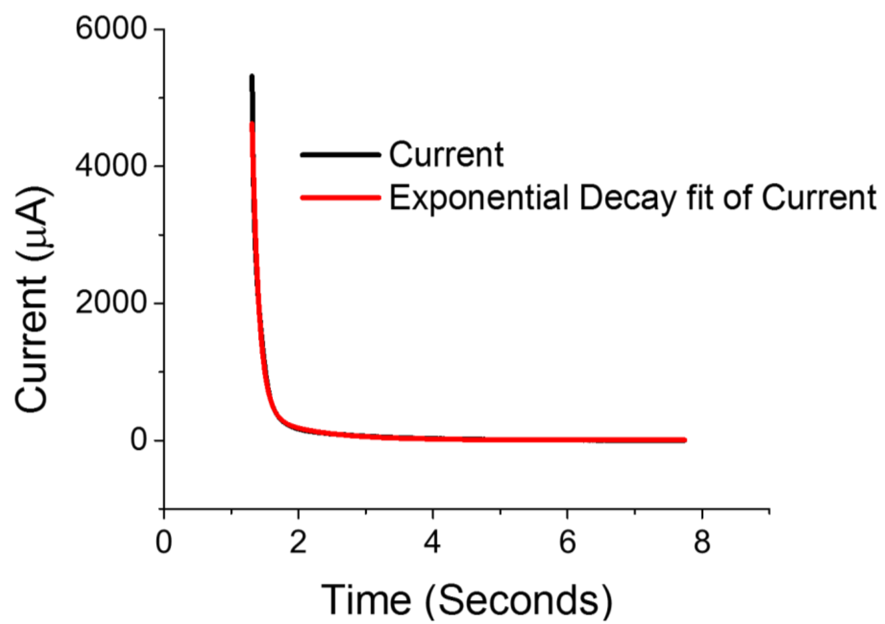

Figure 4.5: Hydrogen oxidation current decay after stepping the potential from -0.25 V to 0 V (black), and the fit of the exponential decay curve (red).

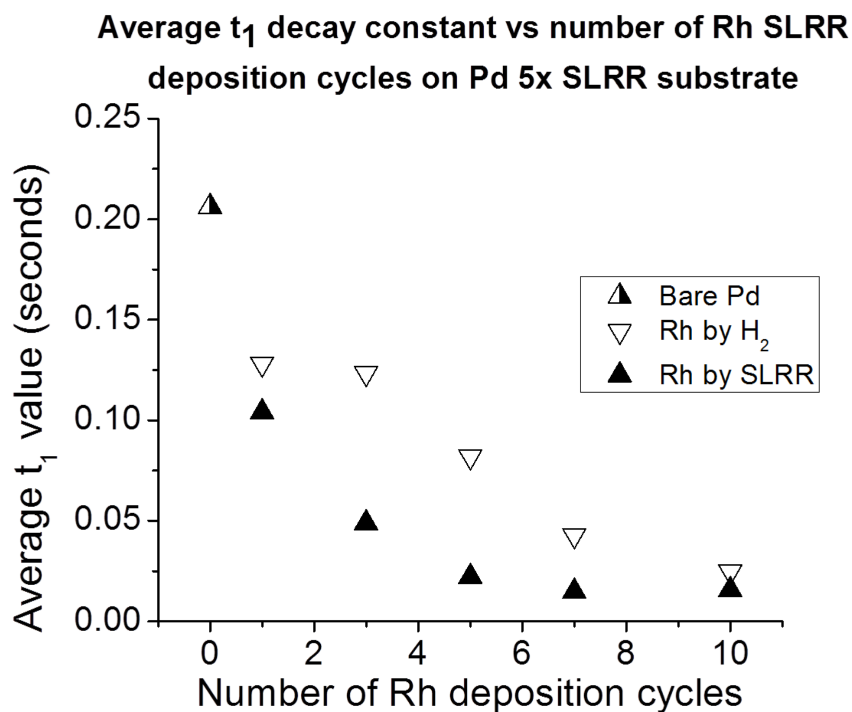

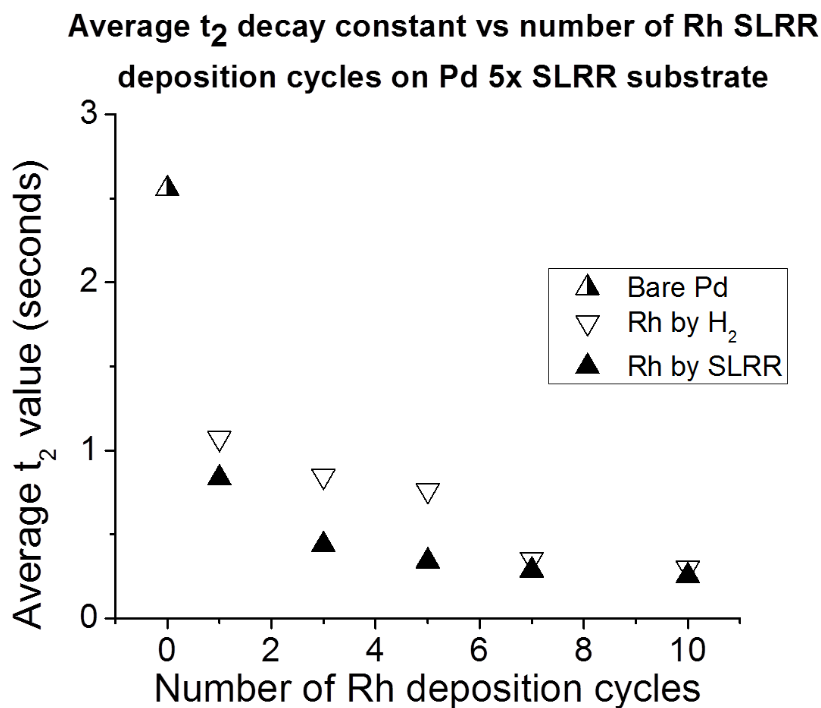

Figure 4.6: Comparison of current decay constants t_1 (top) and t_2 (bottom) of potential step-induced dehydriding currents for varying numbers of cycles of electrochemical ("SLRR") or electroless ("H_2") atomic-layer deposition of rhodium.

CHAPTER 5

ELECTROLESS ATOMIC LAYER DEPOSITION[1]

[1] D. Benson, K. Jagannathan, D. Robinson, and J. Stickney, To be submitted to *Electrochimica Acta (2015)*

Abstract

Electroless deposition methods are examined with the goal of creating atomic layer deposits. Electrochemical atomic layer electroless deposition (EL-ALD) is introduced as a concept. EL-ALD aims to use redox couples in solution to poise the potential where a metal will form a UPD layer to act as a sacrificial metal in a surface limited redox replacement (SLRR). EL-ALD is implemented to use ferricyanide and ferrocyanide solution for Cu UPD followed by exchange for Pd. Stripping voltammetry upon the electrolessly deposited Cu UPD indicates at least 0.7 monolayer is present. Cyclic voltammetry performed on the resulting deposit shows only a minimal amount of Pd deposition. Another electrochemical deposition method is employed that holds the potential in the presence of blank solution, and then goes open circuit prior to flowing in Pt solution to deposit. Cyclic voltammetry shows that the Pt successfully deposits on the Pd, but comparison to Pt grown by E-ALD indicates that the electroless method is much slower at depositing Pt.

Introduction

Several methods of depositing metals with atomic layer control have been presented.[1-4] Electroless deposition methods are advantageous in that they can operate without requiring an instrument to be connected to the substrate,[5] and they do not suffer from limitations due to current input requirements that accompany high surface areas. Electroless deposition as it currently applies to industry typically uses complex and often proprietary solutions to create continuous deposition. These solutions can contain stabilizers, inhibitors, complexing agents, reducing agents, and more.[6] Areas of

improvement to electroless deposition would be making the plating baths less complex, and less expensive.[7]

The method presented here, electroless atomic layer deposition (EL-ALD), has potential to incorporate these desirable qualities. The concept behind this deposition process is that a redox couple in solution, rather than a potentiostat, could poise the potential where a specific element such as Cu will form a surface-limited layer via underpotential deposition (UPD). When a solution containing a more noble metal of interest then flows into the cell, the UPD metal serves as a "sacrificial" element, leaving the surface as the desired metal ions are reduced onto the substrate.[8-11] Pd is one substrate that can benefit from electroless deposition techniques. Pd is attractive for its hydrogen storage capabilities[12] and its catalytic properties.[13,14] Studies suggest that surface modification of Pd substrates with atomic layer deposits of other metals may enhance the surface energetics desired for hydrogen storage and sensing applications.[15] The potential for enhanced kinetics of hydrogen transfer make Pd a compelling target for electroless surface modification techniques.

Experimental

All solutions were prepared using 18 MΩ cm water from a water filtration system (Milli-Q Advantage A10). Pt solution consisted of 0.01 mM H_2PtCl_6 (Fisher, ultrapure grade) with 50 mM $HClO_4$ (J.T. Baker, A.C.S. reagent grade). The sacrificial metal solution for SLRR was 2 mM $CuSO_4$ (J.T. Baker, 99.8%) in 0.1 M H_2SO_4. The blank solution was 0.1 M H_2SO_4 (Fisher, analytical grade). Ferrocyanide solution was 10 mM $K_4[Fe(CN)_6]$ with 0.1 M $NaClO_4$ for a supporting electrolyte and had a pH of 3. Ferricyanide solution was 1 mM $K_3[Fe(CN)_6]$ with 0.1 M $NaClO_4$ and was pH 3. The

stripping solution was 0.1 M HCl (Fischer Scientific). During experiments, and for at least 60 minutes before, solutions were degassed with N_2 to expel dissolved O_2.

Experiments were performed using an automated flow cell system (Electrochemical ALD, L.C.), which consisted of a variable speed pump, solenoid selection valve, solution reservoirs, potentiostat, and a three electrode flow cell (Figure 5.1). The experiments were controlled using Sequencer 4.0 control software (Electrochemical ALD, L.C.). All potentials are reported vs the Ag/AgCl (3 M KCl) reference electrode from Bioanalytical Systems, Inc. Cyclic voltammetry (CV) was performed at a scan rate of 10 mV/sec unless otherwise noted. The gold substrate was polycrystalline gold on glass from Evaporated Metal Films.

Electroless deposition of the Cu was performed by poising the potential of the solution at about 0.16 V vs Ag/AgCl using a ferrocyanide/ferricyanide solution in a molar ratio of 10:1 (Fe^{2+}:Fe^{3+}) for 15 seconds, then flowing in the solution containing both Fe ions and Cu^{2+} ions for 5 minutes at a flow rate of 2 mL/minute before concluding with a 60 second blank rinse. The stripping cycle used a potential sweep from 150 mV to 750 mV at a rate of 5 mV/s in 0.1 M HCl solution.

Pd exchange for Cu was done by flowing in the Pd solution for 15 seconds, then stopping solution flow and allowing the Pd to exchange until the potential reached a predetermined “stop” potential of 0.39 V. The cell was then rinsed with blank solution for 60 seconds. The Cu deposition and Pd exchange were repeated as a cycle a desired number of times.

The electroless deposition of Pt from a poised-potential blank solution began with flowing H_2SO_4 into the cell and holding the potential at 100 mV for 60 seconds. The

voltage was then released to open circuit and Pt solution flowed into the cell for 15 seconds. Solution flow was stopped and the solution was held in the cell for 45 seconds before being rinsed out by blank solution for 90 seconds. These steps were repeated as a cycle the desired number of times to create a deposit.

Results

The proposed mechanism for the EL-ALD cycle using the ferricyanide and ferrocyanide couple depositing UPD Cu and exchanging for Pd is depicted in Figure 5.2. The potential of the solution is poised at about 0.16 V vs Ag/AgCl using a ferrocyanide:ferricyanide (Fe^{2+}:Fe^{3+}) ratio of 10:1. The potential range for Cu UPD has been widely studied, and recent work in this group used 0.15 V to generate Cu UPD.[11,16,17] A solution containing the Fe ions as well as the Cu^{2+} ions is then flowed through the cell to deposit the Cu. A blank rinse removes the excess ions from the cell. The potential is then released to open circuit and Pd^{2+} ions flow into the cell, where they are reduced onto the Au substrate as the less noble Cu sacrifices its electrons and leaves as Cu^{2+} ions. Another blank rinse removes the Pd solution and Cu^{2+} ions from the cell, completing the cycle.

After performing the electroless Cu UPD portion of the cycle, the deposited Cu was stripped from the Pd surface in order to integrate the charge to determine how much had been deposited (Figure 5.3). The area under the curve is about 650 μC, which is then divided by 2 for oxidation of Cu being a 2 e^- process, giving about 325 μC. Dividing again by the area of the electrode, 2 cm^2, yields a final charge density of about 160 $\mu C/cm^2$. For one monolayer of coverage, about 220 $\mu C/cm^2$ is expected.[18] Even if the

peak is extrapolated, the integrated charge from the Cu deposition indicates that less than 1 ML of Cu is being deposited, in good agreement with a successful UPD process.

Once it was established that the electroless UPD of Cu was successful, the next step was to exchange the Cu for a more noble metal, in this case Pd as depicted in Figure 5.2. Cyclic voltammetry was performed on the Au slide after 5 cycles of the EL-ALD Pd deposition (Figure 5.4). A scan rate of 20 mV/sec was used. The most negative portion of Scan 1 (blue) shows excess oxygen due to stagnant solution in the line prior to beginning the CV, and can be ignored. The rest of the scans appear very similar to one another. The peak starting at 700 mV as the scan moves in the positive direction is due to Pd oxide formation, the peak at 1100 after the scan begins moving negative is the Au oxide reduction, and the peak at 700 as the scan continues negative is Pd oxide reduction. The appearance of Pd oxide formation and reduction peaks is indicative of successful Pd deposition, as is the diminution of the Au oxide reduction peak. No H absorption or desorption is observed, which may mean that the Pd has not yet gotten more than one atomic layer thick, as at least 2 layers of Pd are required to absorb H.[19,20] The presence of the Au oxide reduction peak points to incomplete surface coverage, as surface Au still exists.

Figure 5.5 shows Pd generated by electrochemical atomic layer deposition overlaid with the same Pd modified by 10 cycles of electroless Pt deposition. This Pt was generated by holding blank solution at a poised potential prior to allowing the cell to go to open circuit and flowing in the Pt solution to deposit. Periodic spikes in the data occurred due to an issue with the electronics and should not be considered as real data points. The hydrogen waves near 0 V accompany hydrogen adsorption on the Pd

substrate. These waves diminish as the Pd surface becomes obscured by deposited Pt. Additionally, the hydrogen absorption and desorption peaks are more vertical, indicating greater reversibility associated with enhanced H transport kinetics.[21] The peak height indicates that the electroless deposition did not result in as much Pt deposition per cycle as SLRR would generate.

Figure 5.6 is presented so that a comparison can be made between Pt deposited by this poised-potential electroless method and by SLRR. The figure shows a series of overlaid CVs of Pt deposited by E-ALD on a 5 cycle Pd SLRR substrate, the same type of substrate upon which the electroless Pt was deposited. The peaks for hydrogen adsorption are similarly decreased for both SLRR and electroless Pt. The peaks for hydrogen absorption and desorption, however, are much taller and sharper for the SLRR Pt. The sharpness is an indicator of the kinetics of absorption and desorption, with sharper peaks correlating to faster hydrogen transport. The peaks for the 10 cycle electroless Pt do not deviate much from the bare Pd. The conclusion can be made that the electroless method did not deposit as much Pt per cycle as SLRR does. This is not unexpected, as the electroless method provided little driving force for Pt deposition due to the blank solution lacking a method of either maintaining the potential in a range where Pt deposition would occur continuously or providing a sacrificial element.

Conclusion

Redox couples in solution are explored as a method of setting a controlled potential for electroless UPD formation. Electrolessly deposited UPD Cu is shown to be attained using a ferrocyanide/ferricyanide solution. Pd is grown successfully on Au, but the deposition process appears to only put down a minimal amount of Pd. Growth of Pt

on Pd is demonstrated using a poised potential in blank solution before going to open circuit and exchanging the blank for a Pt ion solution, and again is slower than E-ALD growth. Cyclic voltammetry data for both the Pt grown on Pd from poised-potential blank and Pd exchanged for the electroless UPD Cu are shown. The fact that the electroless UPD portion of EL-ALD works is promising. The next step is to figure out a method to get more effective exchange of the Cu for the desired metal.

Acknowledgements

Acknowledgment is made of the support of the National Science Foundation, Division of Materials Research #1410109, and of the Laboratory-Directed Research and Development program at Sandia National Laboratories, a multiprogram laboratory managed and operated by Sandia Corporation, a wholly owned subsidiary of Lockheed Martin Corporation, for the U.S. Department of Energy's National Nuclear Security Administration under contract DE-AC04-94AL85000.

References

(1) Cappillino, P. J.; Sugar, J. D.; El Gabaly, F.; Cai, T. Y.; Liu, Z.; Stickney, J. L.; Robinson, D. B. Atomic-Layer Electroless Deposition: A Scalable Approach to Surface-Modified Metal Powders. *Langmuir* **2014**.

(2) Sheridan, L. B.; Gebregziabiher, D. K.; Stickney, J. L.; Robinson, D. B. Formation of Palladium Nanofilms Using Electrochemical Atomic Layer Deposition (E-ALD) with Chloride Complexation. *Langmuir* **2013**, *29*, 1592-1600.

(3) Ambrozik, S.; Dimitrov, N. The Deposition of Pt via Electroless Surface Limited Redox Replacement. *Electrochimica Acta* **2015**, *169*, 248-255.

(4) Nutariya, J.; Fayette, M.; Dimitrov, N.; Vasiljevic, N. Growth of Pt by surface limited redox replacement of underpotentially deposited hydrogen. *Electrochimica Acta* **2013**, *112*, 813-823.

(5) Brenner, A.; Riddell, G. E. Nickel Plating on Steel by Chemical Reduction. *Journal of Research of the National Bureau of Standards* **1946**, *37*, 31-34.

(6) Mallory, G. O.: The Fundamental Aspects of Electroless Nickel Plating. In *Electroless Plating: Fundamentals and Applications*; Mallory, G. O., Hajdu, J.B., Ed.; Noyes Publications/William Andrew Publishing, LLC: Norwich, NY, 1990.

(7) Sudagar, J.; Lian, J.; Sha, W. Electroless nickel, alloy, composite and nano coatings – A critical review. *Journal of Alloys and Compounds* **2013**, *571*, 183-204.

(8) Brankovic, S. R.; Wang, J. X.; Adžić, R. R. Metal monolayer deposition by replacement of metal adlayers on electrode surfaces. *Surface Science* **2001**, *474*, L173-L179.

(9) Mrozek, M. F.; Xie, Y.; Weaver, M. J. Surface-enhanced Raman scattering on uniform platinum-group overlayers: preparation by redox replacement of underpotential-deposited metals on gold. *Analytical chemistry* **2001**, *73*, 5953-5960.

(10) Vasilic, R.; Dimitrov, N. Epitaxial Growth by Monolayer-Restricted Galvanic Displacement. *Electrochemical and Solid-State Letters* **2005**, *8*, C173-C176.

(11) Herrero, E.; Buller, L. J.; Abruña, H. D. Underpotential Deposition at Single Crystal Surfaces of Au, Pt, Ag and Other Materials. *Chemical Reviews* **2001**, *101*, 1897-1930.

(12) Niessen, R. A. H.; Vermeulen, P.; Notten, P. H. L. The electrochemistry of Pd-coated MgySc(1-y) thin film electrodes: A thermodynamic and kinetic study. *Electrochimica Acta* **2006**, *51*, 2427-2436.

(13) Kang, S.; Heo, P.; Lee, Y. H.; Ha, J.; Chang, I.; Cha, S.-W. Low intermediate temperature ceramic fuel cell with Y-doped BaZrO3 electrolyte and thin film Pd anode on porous substrate. *Electrochemistry Communications* **2011**, *13*, 374-377.

(14) Lai, B.-K.; Kerman, K.; Ramanathan, S. Methane-fueled thin film micro-solid oxide fuel cells with nanoporous palladium anodes. *Journal of Power Sources* **2011**, *196*, 6299-6304.

(15) Greeley, J.; Mavrikakis, M. Surface and Subsurface Hydrogen: Adsorption Properties on Transition Metals and Near-Surface Alloys. *The Journal of Physical Chemistry B* **2005**, *109*, 3460-3471.

(16) Sheridan, L. B.; Czerwiniski, J.; Jayaraju, N.; Gebregziabiher, D. K.; Stickney, J. L.; Robinson, D. B.; Soriaga, M. P. Electrochemical atomic layer deposition

(E-ALD) of palladium nanofilms by surface limited redox replacement (SLRR), with EDTA complexation. *Electrocatalysis* **2012**, *3*, 96-107.

(17) Kim, Y.-G.; Kim, J. Y.; Vairavapandian, D.; Stickney, J. L. Platinum Nanofilm Formation by EC-ALE via Redox Replacement of UPD Copper: Studies Using in-Situ Scanning Tunneling Microscopy. *The Journal of Physical Chemistry B* **2006**, *110*, 17998-18006.

(18) Conway, B. E.; Angerstein-Kozlowska, H. The electrochemical study of multiple-state adsorption in monolayers. *Accounts of Chemical Research* **1981**, *14*, 49-56.

(19) Álvarez, B.; Berná, A.; Rodes, A.; Feliu, J. M. Electrochemical properties of palladium adlayers on Pt(1 0 0) substrates. *Surface Science* **2004**, *573*, 32-46.

(20) Tang, J.; Petri, M.; Kibler, L. A.; Kolb, D. M. Pd deposition onto Au(111) electrodes from sulphuric acid solution. *Electrochimica Acta* **2005**, *51*, 125-132.

(21) Sheridan, L. B.; Yates, V. M.; Benson, D. M.; Stickney, J. L.; Robinson, D. B. Hydrogen sorption properties of bare and Rh-modified Pd nanofilms grown via surface limited redox replacement reactions. *Electrochimica Acta* **2014**, *128*, 400-405.

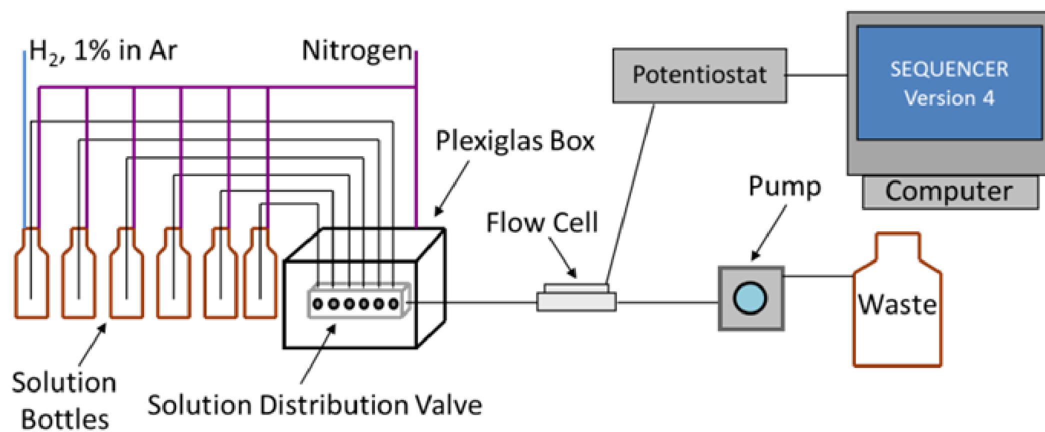

Figure 5.1: Schematic of the flow cell system used for EL-ALD

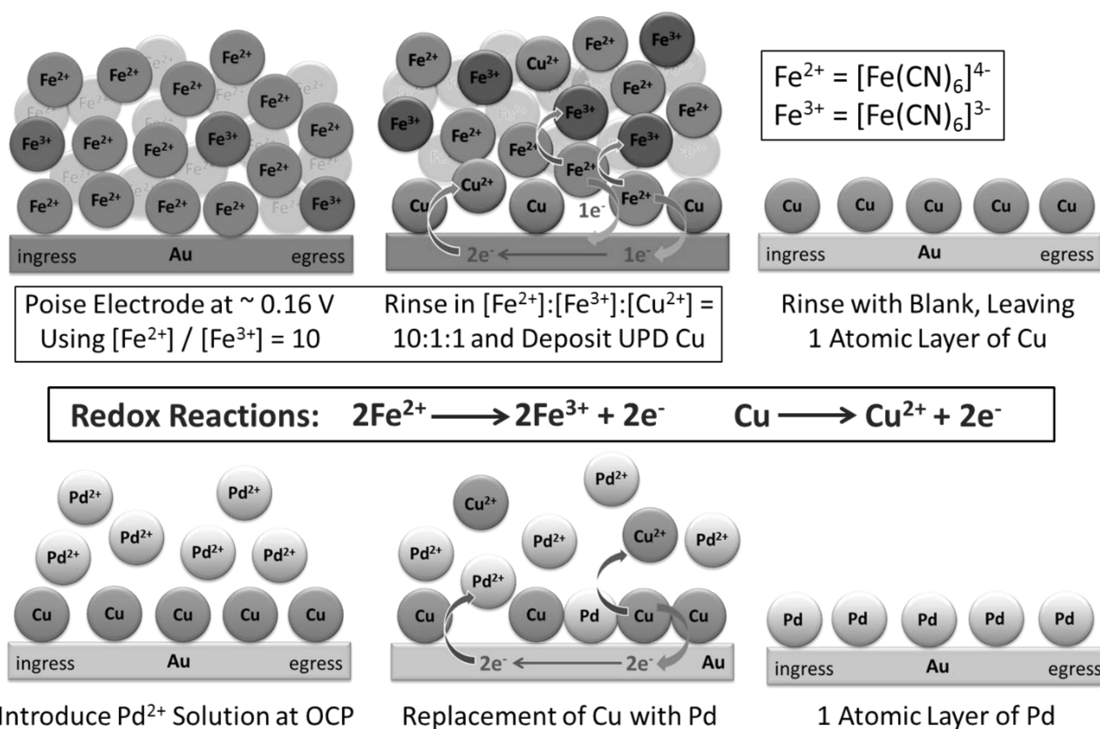

Figure 5.2: Schematic cartoon of EL-ALD mechanism.

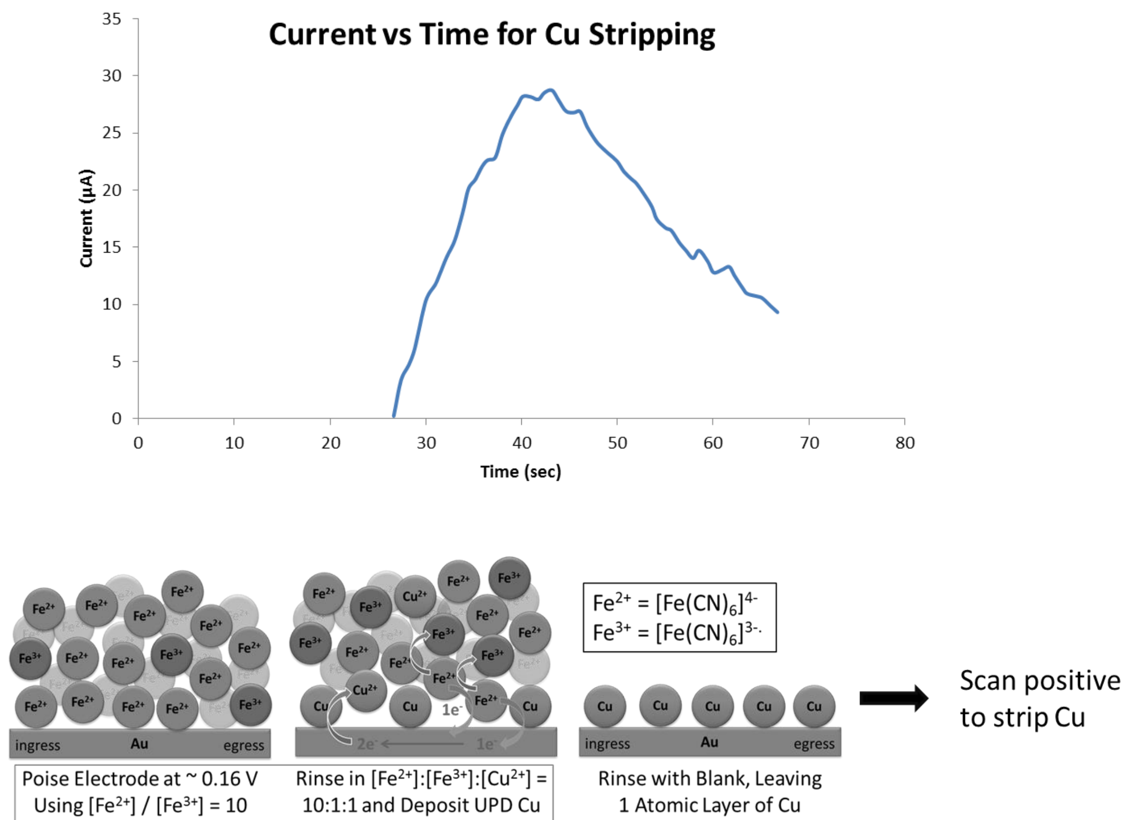

Figure 5.3: Stripping peak for Cu deposited by electroless UPD (top), and schematic diagram of the process leading to the stripping step (bottom).

Pd E-ALD Film Formed by 5 Cycles of Electroless- ALD

CV: 0.1 M H_2SO_4, 20 mV/s

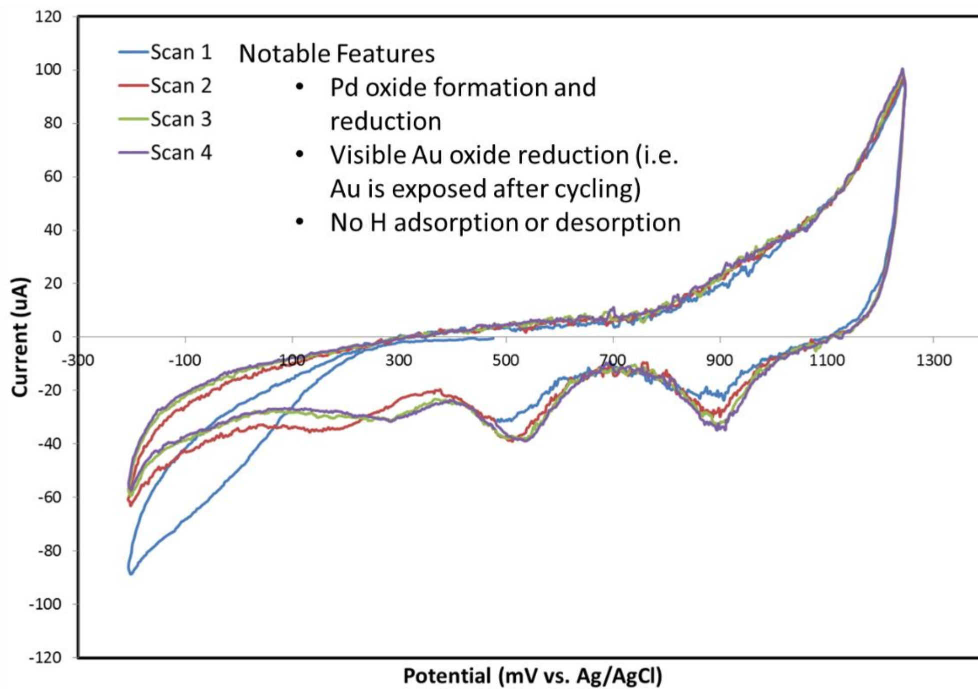

Figure 5.4: CV of Au slide after 5 cycle Pd EL-ALD.

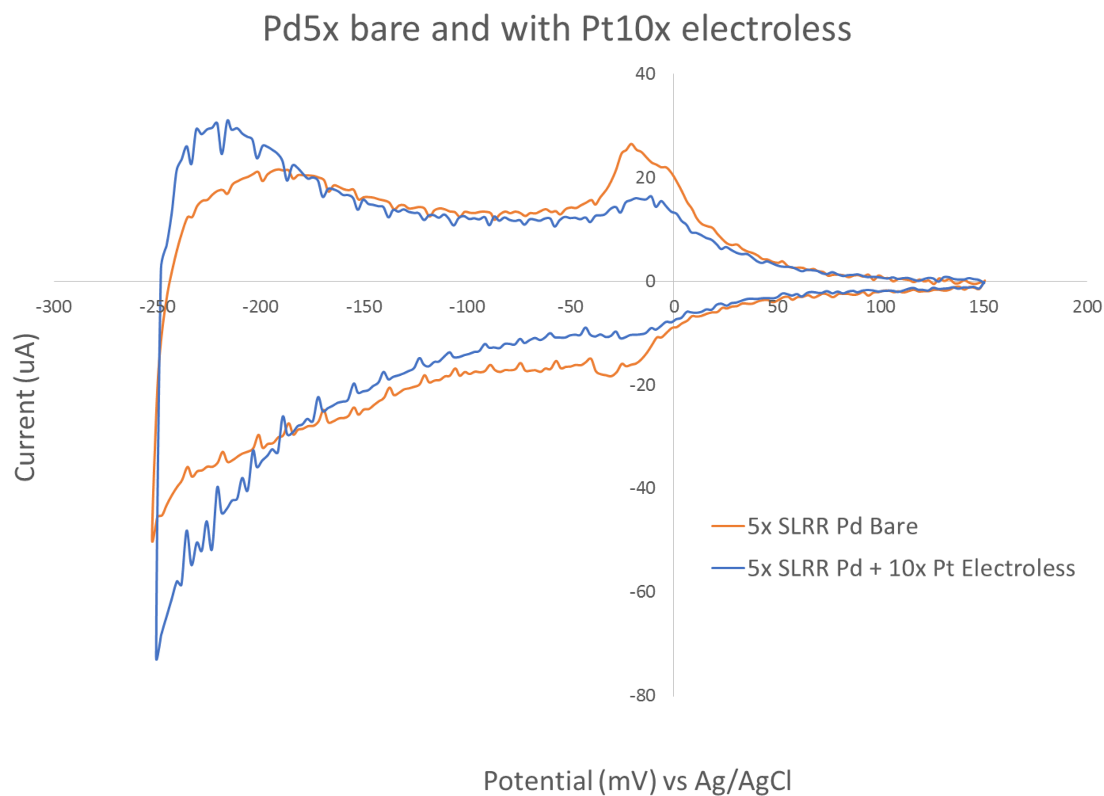

Figure 5.5: CV overlay of a 5 cycle Pd SLRR substrate bare and modified with 10 cycles of electroless Pt deposition.

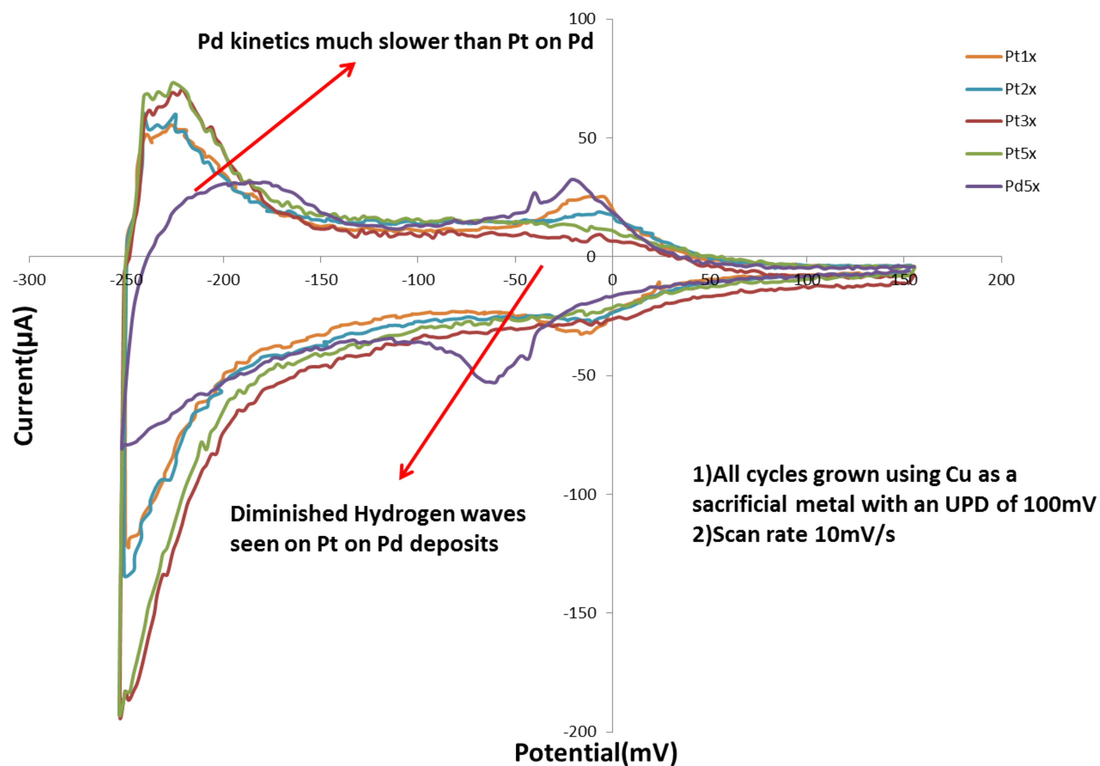

Figure 5.6: CV overlay of a 5 cycle Pd SLRR substrate and 1, 2, 3, and 5 cycles of Pt grown electrochemically on the Pd.

CHAPTER 6

CONCLUSION AND OUTLOOK

The focus of this dissertation was a variety of electroless and electrochemical atomic layer deposition techniques for growing Pd and modifying Pd surfaces with Rh or Pt. Electrochemical atomic layer deposition (E-ALD) and atomic layer electroless deposition (ALED) were both shown to successfully create metal deposits with submonolayer thickness. Electroless atomic layer deposition (EL-ALD) was also studied in an effort to form electroless UPD of sacrificial Cu to exchange for a more noble metal, though more work is needed to make EL-ALD competitive with the other methods.

Chapter 2 examined the adaptation of electrochemical atomic layer deposition (E-ALD) to a powder Pd substrate. A new flow cell design was implemented to facilitate deposition on powders. Both Rh and Pt were shown to be effectively deposited in a layer by layer method on the Pd powder. Cyclic voltammetry indicated that kinetic enhancement in the rate of hydrogen sorption and desorption could be observed on mg-scale quantities of power modified with Rh although they could not be observed for the bulk 300 mg samples. X-ray photoelectron spectroscopy (XPS) indicated increasing deposit thickness with increasing deposition cycles. Scanning transmission electron microscopy with energy dispersive X-ray spectroscopy (STEM-EDS) on microtomed powder particles was used to generate elemental maps that showed conformal deposition on the powder surface regardless of morphology.

Chapter 3 focused on adapting an electroless analog to E-ALD, called atomic layer electroless deposition (ALED) to the flow cell system. Hydride formation was optimized using solution flow containing dissolved H_2 in blank. Using cyclic

voltammetry, ALED was shown to be effective in creating deposits of Rh on a Pd substrate as well as Pd on a Pd seed layer generated by SLRR. Cyclic voltammetry also showed consistent characteristics with layer-by-layer control over growth. ALED was found to deposit less material per cycle than E-ALD.

Results from Chapter 4 were based on a comparison of deposits made in the flow cell system by E-ALD and ALED. Voltammetric stepping experiments were used to generate desorption profiles as hydrogen left the Pd. Decay curve fitting allowed comparison of time constants for desorption. Deposits of Rh on Pd created by both E-ALD and ALED showed faster desorption with increased Rh deposition cycles. ALED was again shown to deposit less Rh per cycle than E-ALD in terms of thickness, and was also found to generate less surface coverage per deposition cycle.

Chapter 5 examined preliminary studies into electroless deposition techniques. Pt deposits were created on a Pd substrate at open circuit after applying a poised potential in blank solution before flowing in the Pd ions. It was shown that electrochemical redox pairs offer possibility for controlled atomic layer deposition. UPD Cu was deposited using a ferricyanide/ferrocyanide solution. Exchange for Pd ions provided less exchange than was expected as evidenced by CV. Electroless atomic layer deposition (EL-ALD) requires further attention in order to optimize the exchange of desired metal ions for the sacrificial metal.

There are several avenues for future work. Other powder substrates or nanostructured materials may be a target for E-ALD now that it has been shown possible to deposit on high-surface area materials. Deposition of materials for photovoltaics on powder would be one such target. Deposition of other metals such as Ru on Pd powder

can also be performed to examine kinetic effects upon hydrogen transport. Electroless deposition methods leave much room to expand. ALED could be performed on powders in the flow cell system to yield a comparison to samples created by E-ALD. Scale-up of the E-ALD on powders is desirable, but would require a larger flow cell, counter electrode, and more current. ALED may be more useful at large scales due to the potential difficulty of increasing current. EL-ALD should be probed in order to facilitate exchange of electrolessly deposited UPD Cu for other metals. The Rh modified Pd has yet to be examined for a maximum surface coverage, but it is expected that at some point the surface would become sufficiently obscured to hinder hydrogen absorption.